PHILOSOPHICAL TRANSACTIONS OF THE ROYAL SOCIETY A MATHEMATICAL, PHYSICAL & ENGINEERING SCIENCES

The Mam Tor Landslide, North Derbyshire

A. W. Skempton, A. D. Leadbeater and R. J. Chandler

Phil. Trans. R. Soc. Lond. A 1989 **329**, 503-547
doi: 10.1098/rsta.1989.0088

Phil. Trans. R. Soc. Lond. A **329**, 503–547 (1989) [503]
Printed in Great Britain

THE MAM TOR LANDSLIDE, NORTH DERBYSHIRE

By A. W. SKEMPTON[1], F.Eng., F.R.S., A. D. LEADBEATER[2] and R. J. CHANDLER[1]

[1] *Department of Civil Engineering, Imperial College of Science and Technology, Exhibition Road, London SW7 2BU, U.K.*
[2] *Derbyshire County Council, Matlock DE4 3AG, U.K.*

(*Received* 5 *August* 1988)

[Plates 1 and 2]

CONTENTS

The ancient but still active landslide at Mam Tor, in Namurian mudstones, is a massive example of a slump-earthflow. It has a length of 1000 m, a maximum width of 450 m, and an average slope of 12° from the toe to the foot of the back scarp. The upper, slump sector has moved about 160 m on a curved slip surface within a shear zone of brecciated clay; the shear zone, 2 m thick and in places at a depth of 30 m, lies above hard mudstone of the Edale Shales; weathered mudstone and any superficial deposits, and several metres of unweathered mudstone, having been removed by shearing and incorporated in the slide debris. By contrast the lower, earthflow sector, which is up to 18 m in thickness, has spread downslope by at least 400 m with little disturbance of the original ground. The landslide probably started about 3600 years ago as a sudden large slip in the steep hillslope. Degradation and softening of the slip mass would rapidly lead to secondary slips and initiation of the earthflow. Subsequent movements can be attributed to a succession of slips, becoming smaller with time, in response to winter rainstorms. Radiocarbon dating of an Alder root in fossil soil beneath the earthflow demonstrates that the cumulative effect of such slips has resulted in the landslide toe advancing 320 m during the past 3200 (± 200) calendar years.

A static analysis of stability shows the slide to be in a state of limiting equilibrium under normal winter groundwater levels, with a residual strength on the slip surface represented by an angle of shearing resistance $\phi'_r = 14°$; a value in good agreement with tests on clays of similar composition. However, records of movements in the present century indicate that slips leading to displacements typically of about 0.3 m are still taking place, an average at four-year intervals, in winter months with more than 200 mm rainfall. An analysis of the mechanics of these 'storm-response' movements is given in terms of the transient rise in water level and the reaction of residual shear resistance to increasing rates of displacement.

Some other large Pennine landslides in Namurian mudstones are known to be considerably older than the Mam Tor slide, and on examination they are found to be permanently stable. By analogy with Mam Tor, this condition has been attained after a long sequence of secondary slips leading progressively to more stable configurations in which reactivation occurs only in heavier (and less frequent) rainfall, until finally the slide mass remains stable even in the most severe rainstorms. The timescale for this process to be completed appears to be of the order of 8000 years.

1. Introduction

The landslide, at the head of Hope Valley near Castleton, north Derbyshire, is of the slump-earthflow type (according to the classification by Varnes (1958)) characteristic of several large slides in mudstones of the Millstone Grit or Namurian Series in valleys of the Pennine hills. It has been investigated by deep boreholes and piezometers, and radiocarbon dating permits an estimate to be made of its age. Records of movements and rainfall are available from 1915 to 1980. Comparisons are drawn with other landslides of similar type and scale; some of considerably greater age and one, in South Wales, of very recent origin.

2. Geology

Mam Tor is the name given to the highest point, surrounded by the ramparts of a prehistoric hillfort, on a sandstone ridge running between Hope Valley, to the south, and Edale, to the north. A plan of the landslide (figure 1) shows geological boundaries, including a fault line, as mapped by Stevenson (1972). The sections (figures 2 and 3) show about 100 m of Mam Tor

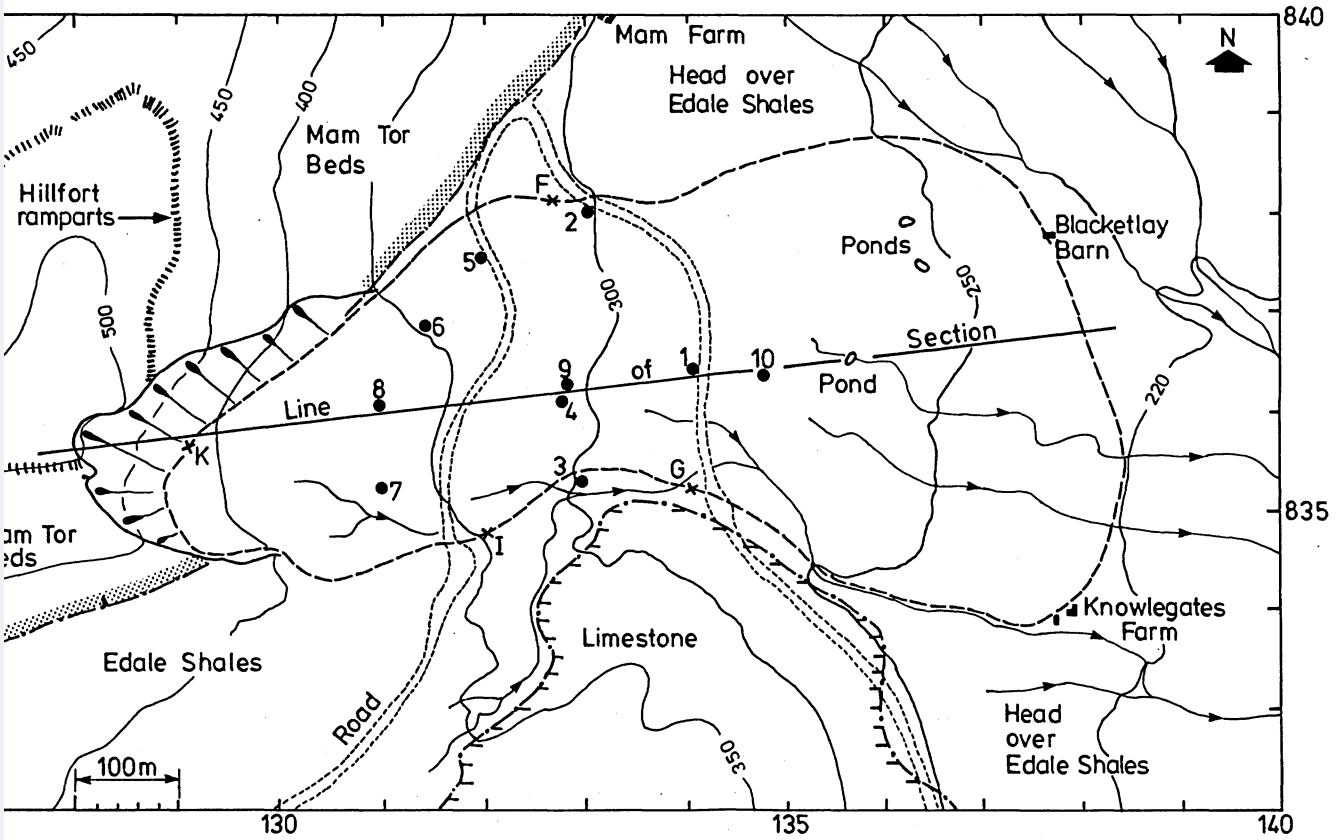

FIGURE 1. Plan of Mam Tor landslide.

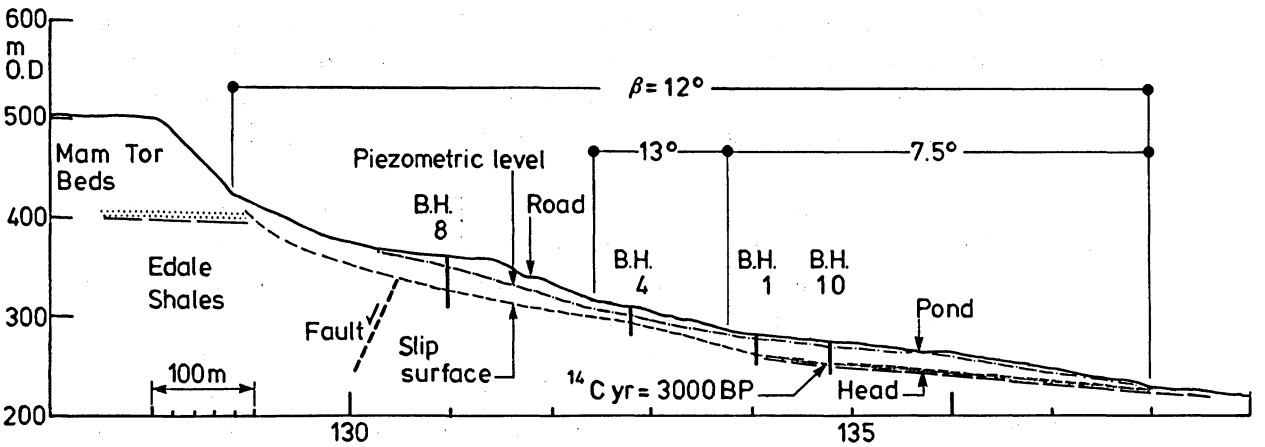

FIGURE 2. Longitudinal section (B.H. is borehole).

Beds overlying Edale Shales, the lowest unit of the Millstone Grit Series (Namurian). Carboniferous limestone outcrops a short distance south of the landslide.

The Mam Tor Beds consist of grey micaceous sandstone alternating with subsidiary siltstone and shale. At the north end of the landslide scarp the beds are seen to be dipping approximately NNE at 8°. By projection of their base plane southwards the downthrow at the fault is found to be about 30 m. The fault dies out before reaching the north boundary of the slide, as it does

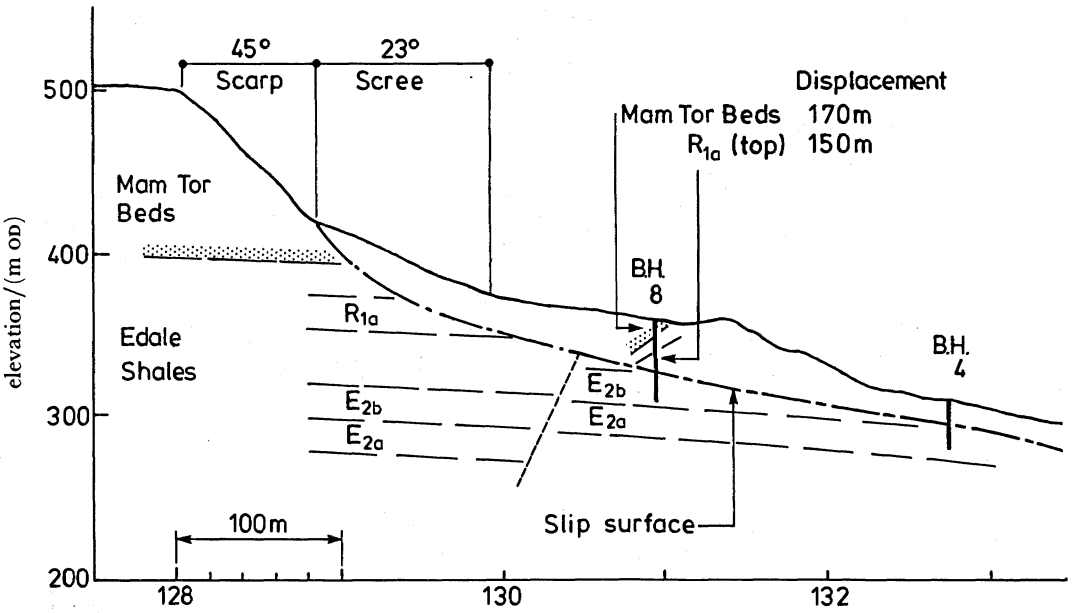

FIGURE 3. Details of slump and scarp.

also 1.5 km to the west, but is still present on the line of section (figure 3) where the downthrow is estimated at 15 m. Flow of groundwater, averaging 0.4 l s^{-1}, from a spring some 70 m southwest of borehole 7 is considered to come from the fault zone (Vear & Curtis 1981).

The Edale Shales in their unweathered state are hard dark grey mudstones with occasional bands of siltstone and ironstone. Pyrite occurs at several horizons, generally in the form of scattered crystalline aggregates. Cores from boreholes can be split along bedding planes at intervals rarely less than 1 cm and often at 10 cm or more. Below obviously weathered material the mudstones are weakened by fissures to a depth of the order of 10 m; an effect indicated by only moderately good core recovery (table 1) and resulting probably from stress release during valley formation, perhaps accentuated by permafrost action in the last (Devensian) glacial period.

Stratigraphic zones, denoted by symbols E_{1a}, E_{1b}, etc. (figure 4), can be identified by distinctive goniatite fossils. Dips of the bedding planes vary from 10° to 20° with a tendency to increase in southerly and easterly directions due partly to differential compaction above an unconformable contact on the underlying limestone.

The sections in figures 3 and 5 are derived from measured dips and identification of goniatite zones in the core samples, coupled with thickness of the zones as given by Stevenson & Gaunt (1971), chiefly from observations in Edale, with some minor changes based on the present investigations. This set of data is self-consistent, establishing the stratigraphy within acceptable limits of accuracy and demonstrating (as might be expected) that the rocks beneath the landslide have not been shifted from their natural position.

To a depth of about 2.5 m below superficial Head deposits the mudstones are weathered to a softer consistency and oxidized on vestigial bedding planes and fissures. Within this depth they are also considerably disrupted, resulting in a core recovery little better than that for the highly disturbed landslide debris (table 1).

South of the landslide the limestone rises from beneath the Shales to form an extensive

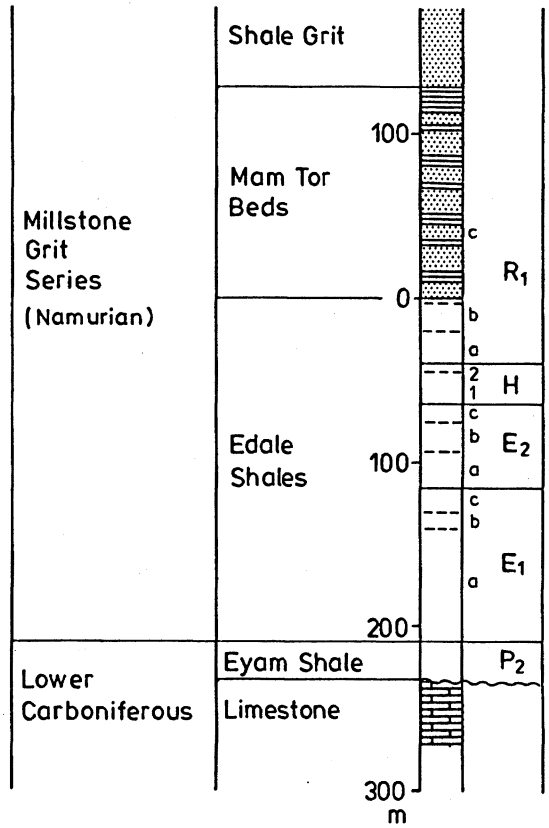

FIGURE 4. Stratigraphy.

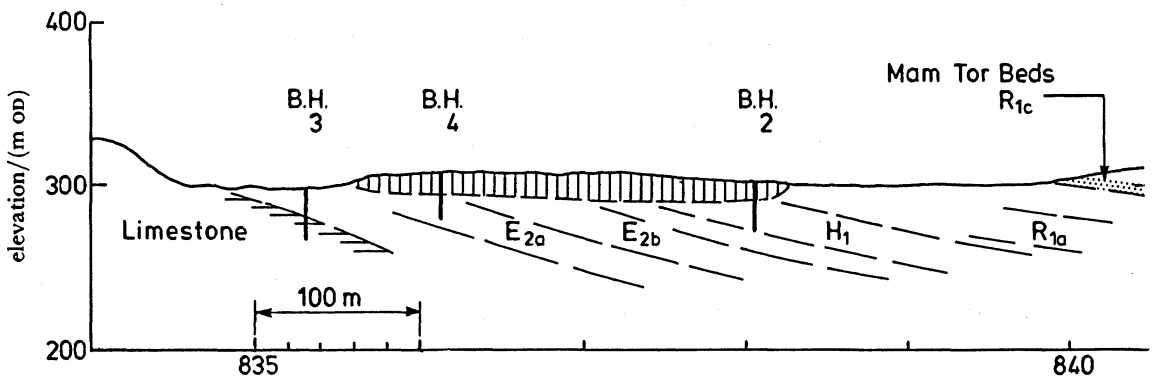

FIGURE 5. Transverse section on grid line 133.

TABLE 1. CORE RECOVERY

(Cores 108 mm nominal diameter taken by water-flush diamond drilling.)

material	numbers of cores	total core recovery (%)
landslide debris	72	70
weathered mudstone	7	78
unweathered mudstone:		
0–8 m } below base of weathering	23	88
8–15 m } below base of weathering	13	94

plateau at around 400 m Ordnance Datum (OD). Scattered erratics on the plateau and patches of glacial till further south, near Bakewell, are remnants of early glaciations (Bureck 1985). But it is certain that the Castleton area and valleys to the north such as Edale, Snake Pass and upper Longdendale, all with massive landslides, have been ice-free since the last (Ipswichian) Interglacial; i.e. for at least 125000 years. Tills of the Devensian glaciation are banked against the west flank of the Pennines, at these latitudes, to a height not above 300 m OD and at a distance more than 5 km from Mam Tor; to the north and east the nearest Devensian till is some 40 km away, and there is none to the south (Geological Survey 1977).

However, during this period (terminating about 11000 years ago) the area would have been subjected to periglacial conditions. These probably account for disruption of the weathered mudstone, by cryoturbation, and were undoubtedly responsible for the valley sides being blanketed by Head: a layer or layers of clay with mudstone and sandstone fragments caused to move downhill, even on quite gentle slopes, by the freeze–thaw process of solifluction.

In Edale and Hope Valley the Head is mapped by Stevenson & Gaunt (1975) as extending over the Edale Shales, from about the 300 m contour to the valley floor. On steeper slopes in the Mam Tor Beds it is perhaps no more than a thin veneer.

Beneath the toe of the Mam Tor landslide Head is exposed above weathered mudstone in a stream bed 100 m west of Knowlegates Farm (figure 1). At a higher altitude, around 250 m OD, a good example is seen in borehole 10. Here, lying undisturbed on a 5° slope, is 2.7 m of grey clay containing fragments of sandstone. Still higher, at 262 m OD in borehole 1, the Head has partly been removed by shearing but 1.2 m remains as mottled clay with sandstone and mudstone fragments. The sandstone fragments must have been transported downhill from the Mam Tor Beds, as the underlying mudstones at both locations contain no sandstone.

In post-glacial times the landscape has changed little, except for landslides. The larger streams have eroded into or through the Head, depositing alluvium in their lower reaches, and on high ground hill peat began forming some 7000 years ago (Tallis 1964).

3. Description of the landslide

(*a*) *Dimensions*

From the crest of the scarp, at 500 m OD, to the toe of earthflow the landslide has a length of 1000 m, a height of 280 m and covers an area of 34 hectares. Its maximum width is about 450 m. From the foot of the scarp to the toe the average slope of the slide mass $\beta = 12°$. On the basis of topography and results of borehole exploration four sectors can be recognized.

(*b*) *Scarp and scree*

On the line of section (figure 3) the scarp face stands at an average slope of 45° to a height of 80 m in Mam Tor Beds. Over the entire face of the scarp the slopes (measured between contours at 10 m vertical intervals) range from 40 to 51°. At its foot, scree extends down to the 370 m contour at an average slope of 23° (range 18–28°); formed of material eroded from the scarp. Gently sloping ground in front of the scree (figure 6, plate 1) is probably composed of fine-grained hillwash sediment. Retreat of the scarp edge by erosion has opened a 100 m gap in the hillfort ramparts (figure 1).

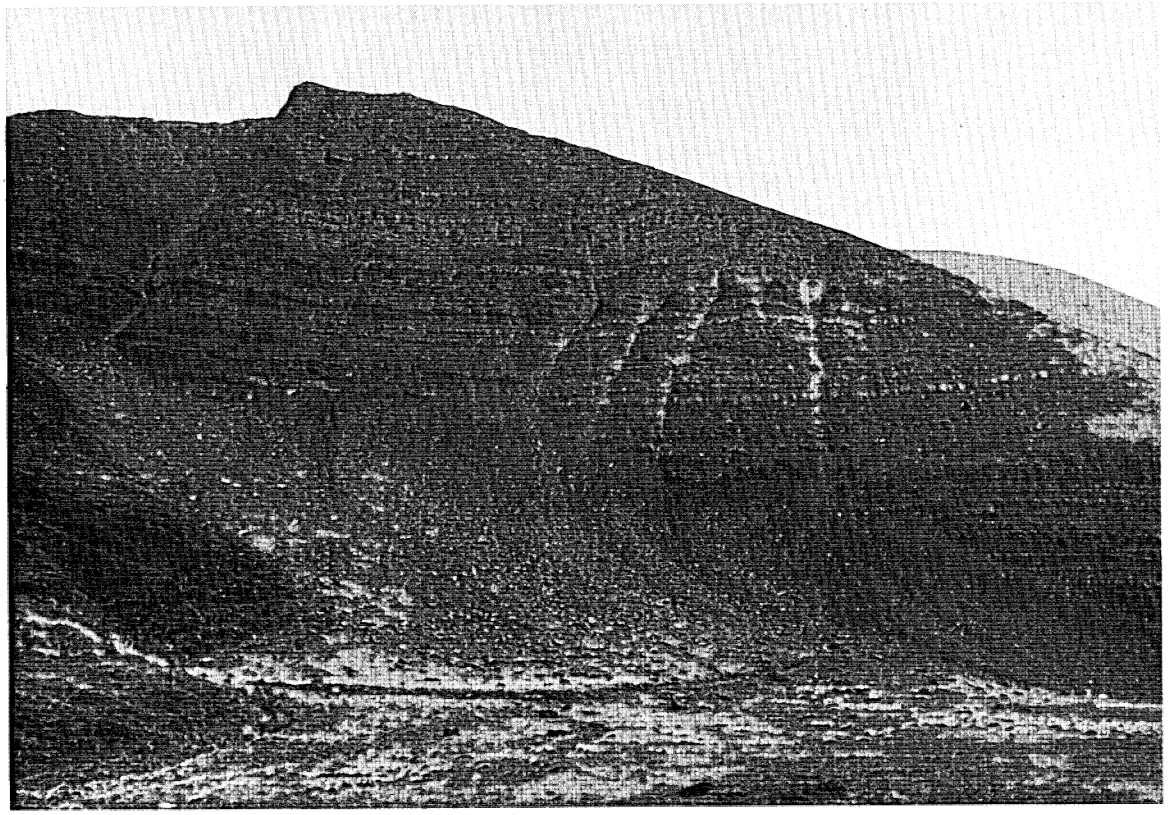

FIGURE 6. Scarp and scree slope.

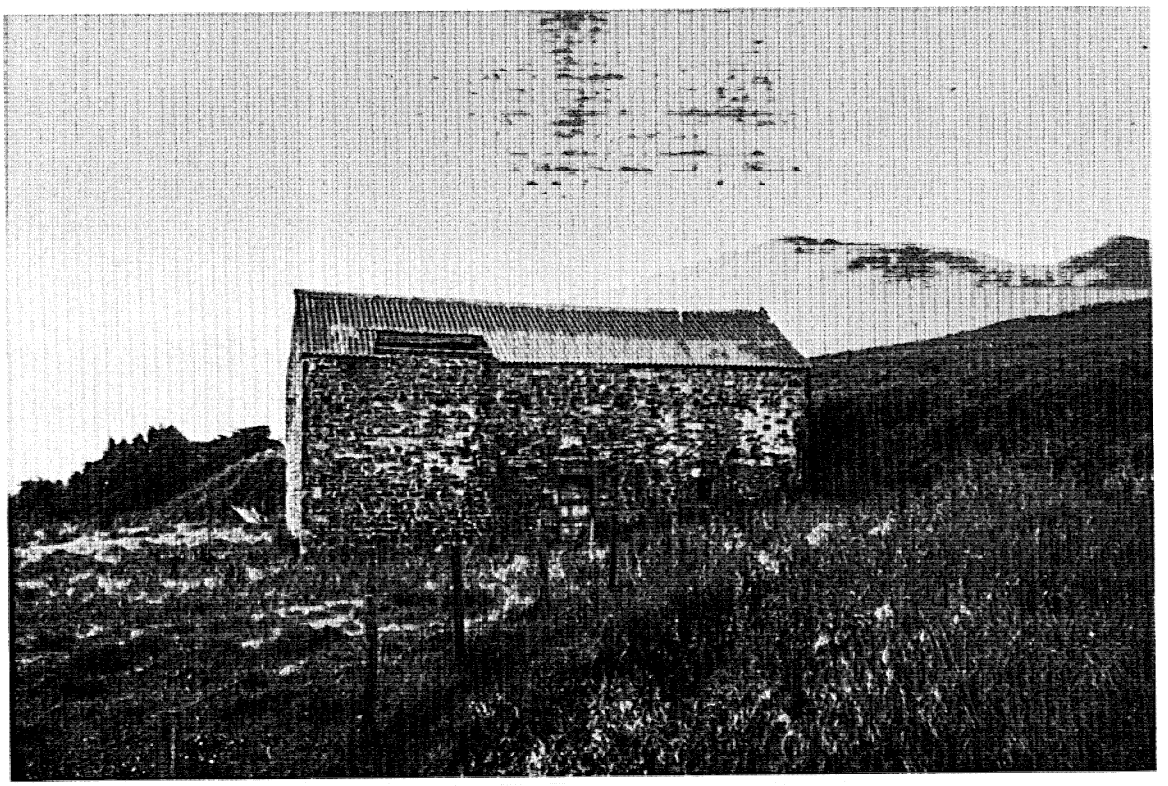

FIGURE 10. Toe of earthflow at Blacketlay Barn.

(*Facing p.* 508)

PHILOSOPHICAL TRANSACTIONS OF THE ROYAL SOCIETY A MATHEMATICAL, PHYSICAL & ENGINEERING SCIENCES

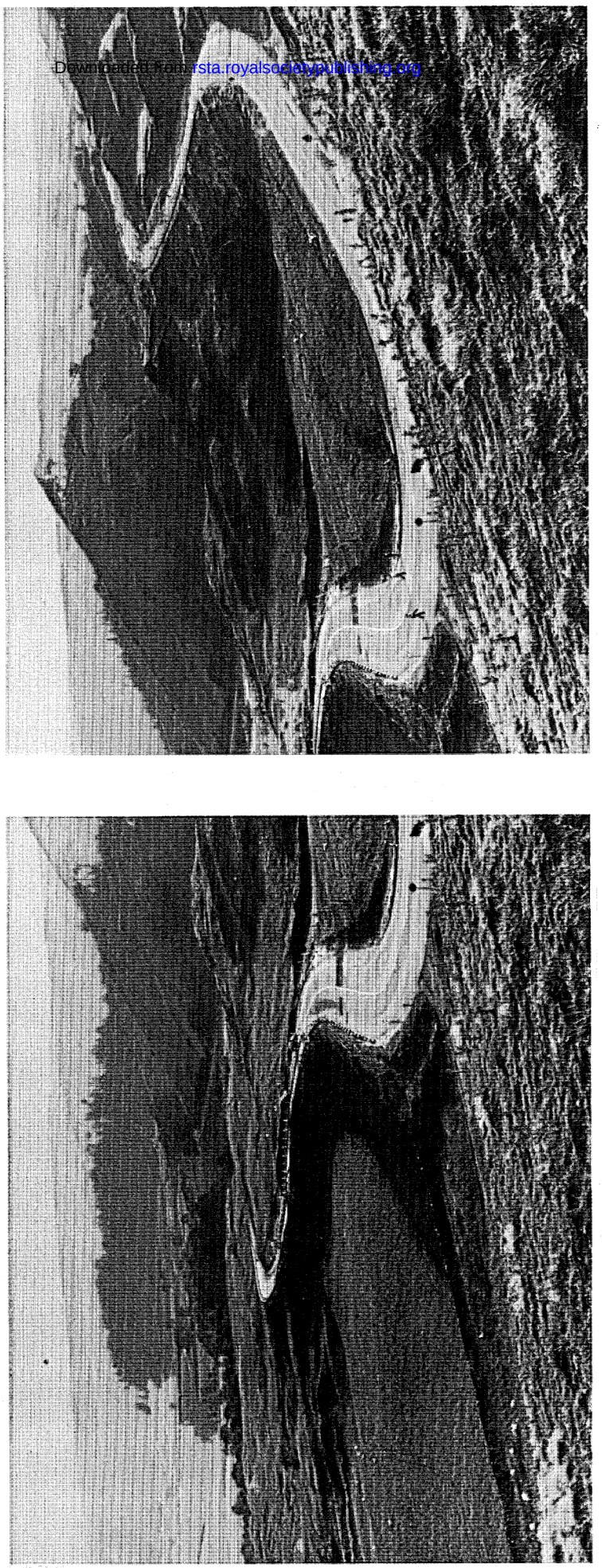

FIGURE 7. Views of landslide, looking south.

PHILOSOPHICAL TRANSACTIONS OF THE ROYAL SOCIETY A MATHEMATICAL, PHYSICAL & ENGINEERING SCIENCES

(*c*) *Slump*

The 'slump' sector of the landslide extends to about the 310 m contour, close to boreholes 2 and 4. Movements have occurred on a curved slip surface with evidence, from boreholes and slump blocks, of back-tilted strata dipping at angles from 30 to 50°. Except where covered by hillwash the slump mass has very irregular topography, as can be seen above and below the road in figure 7, plate 2, and the front slopes vary from 14 to 25°.

Borehole 8 (figure 8) is the principal source of information on the structure of the slump. Two polished and striated slip surfaces, 10 cm apart, are found near the base of 2.6 m of brecciated

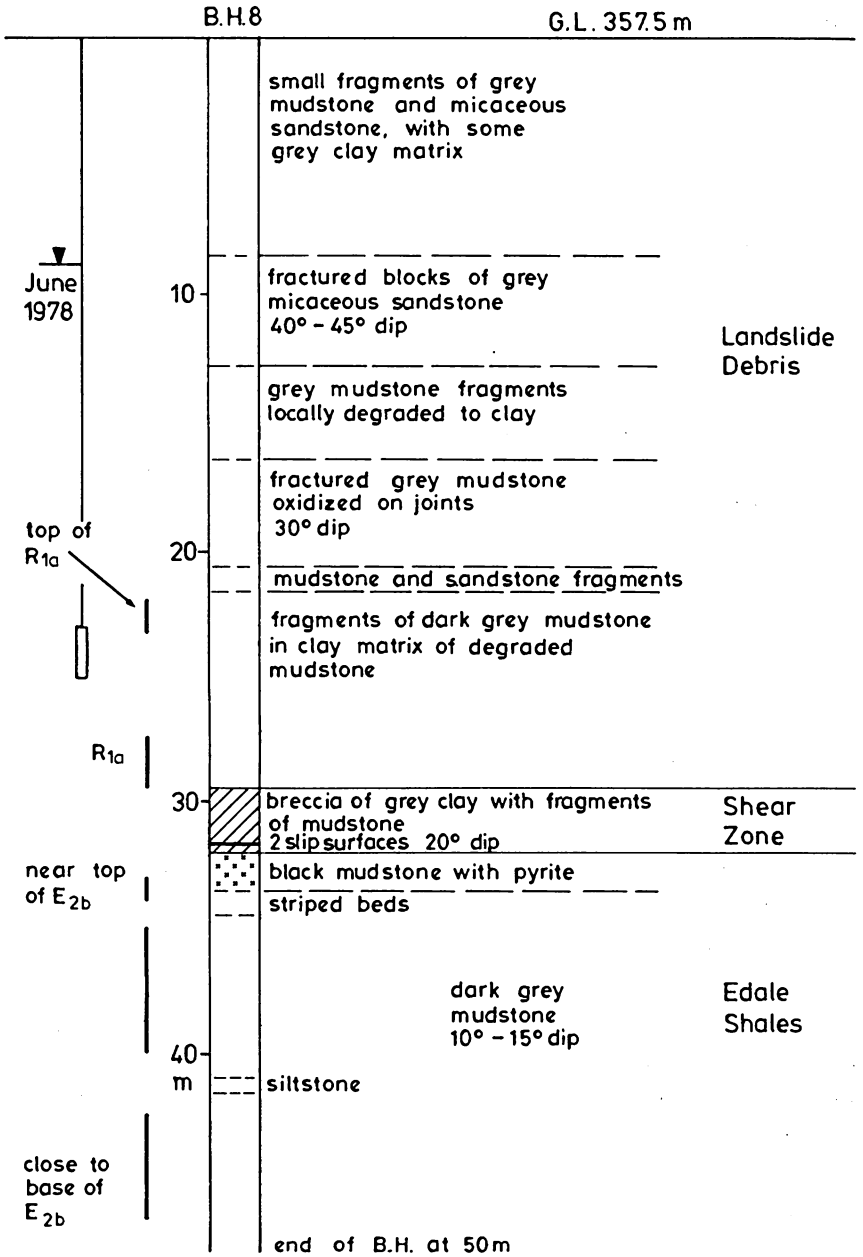

FIGURE 8

clay 32 m below ground level. This shear zone lies immediately above unweathered mudstone notable for excellent (98%) core recovery. Thus the entire thickness of weathered mudstone and any superficial deposits, and probably at least 8 m of unweathered mudstone as well, have been removed by shearing.

Lengths in which goniatite zones can be identified are indicated on the left-hand side of figure 8. The 18 m of mudstone penetrated in this borehole encompass practically the whole thickness of zone E_{2b}.

Landslide debris above the shear zone includes pieces of mudstone from the top of zone R_{1a}, and 10 m above are blocks of grey micaceous sandstone of the Mam Tor Beds back-tilted at 40–45°. Though broken and disturbed, and missing a portion of zone R_{1b}, the rocks are recognizably in their proper sequence, and demonstrate a displacement along the slip surface of approximately 160 m (figure 3).

Borehole 6, 80 m north of the line of section, shows a shear zone of brecciated clay 2.9 m thick, at a depth of 21 m, again directly above unweathered mudstone which at this location belongs to zone H_{1a}. Only six of the nine cores in the mudstone have a good degree of recovery, perhaps indicating that shearing is not so deep below original ground level as at borehole 8. About 50% of the landslide debris in borehole 6 is composed of blocks and fragments of Mam Tor sandstone, some of which show up to 35° back-tilt. Borehole 5, further northwest but still within the slump penetrated 20 m of slide debris containing fragments of sandstone and R_{1b} mudstone above fragments of zone R_{1a} in a clay matrix of completely degraded mudstone. It failed to reach the shear zone. This was the case also at borehole 7, in the south part of the slump, where to a depth of 29 m there are broken and disrupted blocks and fragments of Mam Tor sandstone, siltstone and shaly mudstone with a sparse clay matrix.

(*d*) *Transition sector*

In this part of the landslide the foot of the slump is transformed into the head of the earthflow. Topography is less irregular, but the slopes are still quite steep, ranging from 9 to 16°, and transverse compression ridges can be seen. The shear zone, at a relatively shallow depth, lies on or a little below the top of the weathered mudstone.

Borehole 4 (figure 9) shows a shear zone of brecciated clay 1.8 m thick with a thin layer of intensely sheared clay at its base, 11.8 m below ground level. This is followed by 2.2 m of weathered, disrupted mudstone. The borehole continues in unweathered pyritic mudstone and, below a minor fault, in mudstone of zone E_{2a}. Core recovery in the unweathered mudstone here, and in the boreholes subsequently described, is not better than about 90% (table 1). Near the base of the landslide debris is an Alder root, radiocarbon dated 860 years before present (BP) and presumably entrained in secondary slips long after the early landslide movements. Borehole 9 was made nearby to install a piezometer.

In borehole 2, also within the transition sector, two slip surfaces 30 cm apart are found in a 50 cm layer of softened mudstone, above 1.8 m of oxidized and iron-stained mudstone. Evidently, shearing has occurred near the top of the weathered mudstone. The lowest 12 m of the borehole passes through the full thickness of zone H_{1a} with a uniform dip of 14°. The slide debris consists chiefly of mudstone fragments in a clay matrix, some of the largest pieces showing a (back-tilt) dip around 35°.

PHILOSOPHICAL TRANSACTIONS OF THE ROYAL SOCIETY A MATHEMATICAL, PHYSICAL & ENGINEERING SCIENCES

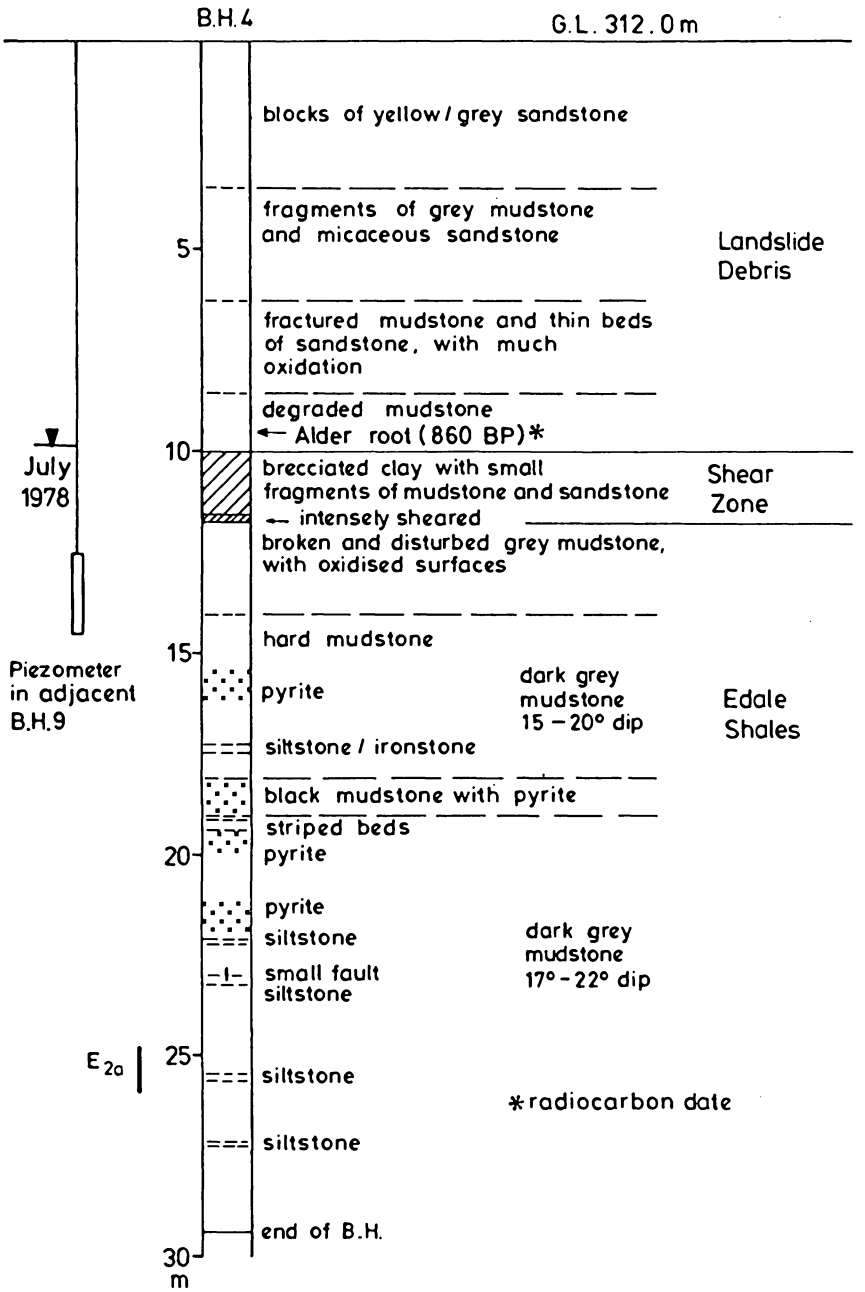

FIGURE 9

(*e*) *Earthflow*

The earthflow extends for a length of about 420 m reaching, at its lowest point, to the 220 m contour. The slope varies between 6 and 9°, the average of 15 measurements being 7.5°. This part of the landslide has moved in almost pure translation by sliding on or just below original ground surface. Consequently, it stands above adjacent ground level with a clearly defined edge and toe (figure 10, plate 1). The surface is hummocky, with a tendency for transverse ridges to be present in the upper parts of the earthflow, and contrasts strongly with

the smooth natural slope alongside. The plan (figure 1) shows that downslope movement of the earthflow has been accompanied by lateral expansion; its width reaches 450 m compared with 250 m in the slump. The earthflow is also characterized by a high winter groundwater level. There is much marshy vegetation and ponds exist in local depressions; three are mapped in figure 1.

In borehole 1 (figure 11) the top of the shear zone is not well defined owing to drilling disturbance and poor core recovery. Signs of a slip surface can be detected in yellow-brown clay at a depth of 17.1 m, and from 17.3 to 17.5 m there is highly brecciated clay containing small fragments of mudstone and sandstone. This can be interpreted as sheared Head. It is underlain

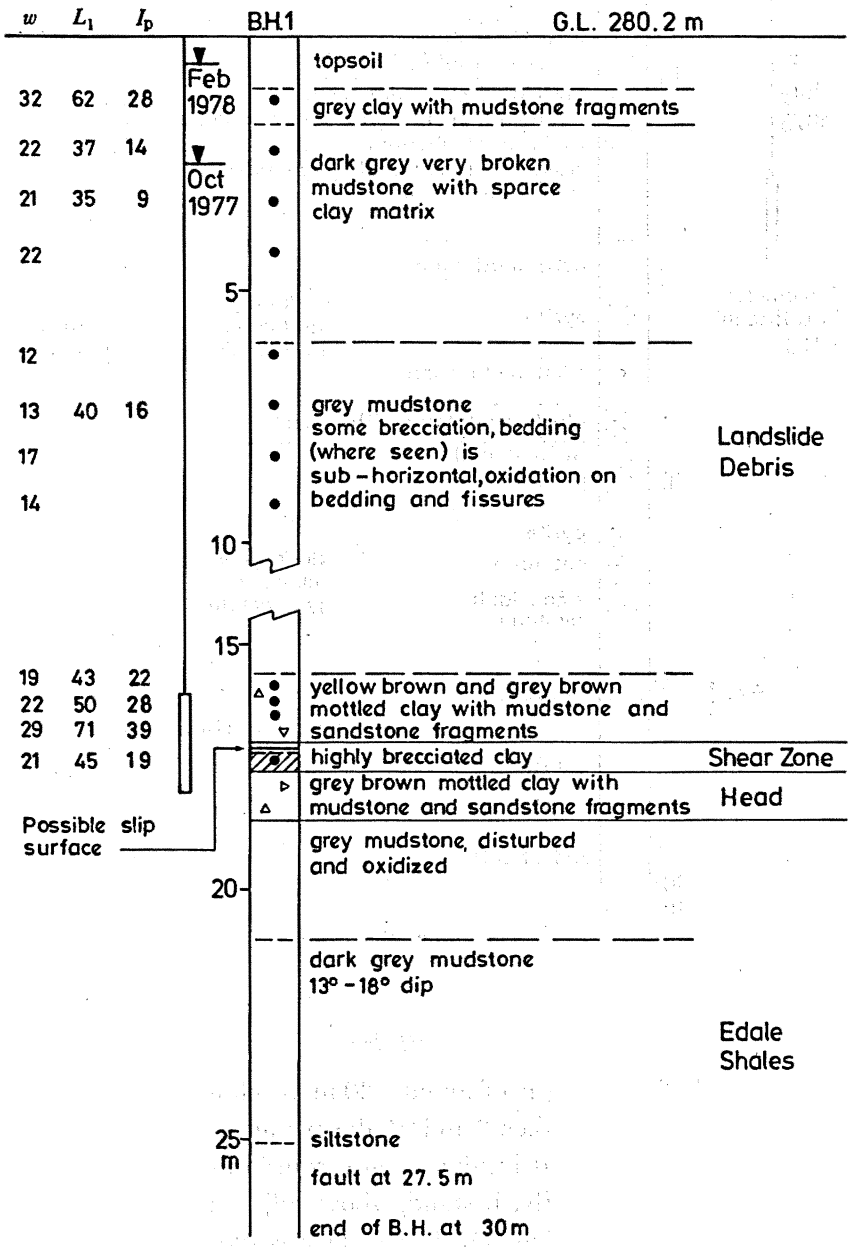

FIGURE 11

by 1 m of unsheared Head consisting of mottled clay with mudstone and micaceous sandstone fragments, followed by about 2.2 m of weathered and disrupted mudstone. A fault plane, dipping at 50°, occurs at 27.5 m and the mudstone is distorted for about 1 m above and below. The slide debris to a depth of 15.5 m is mudstone in varying degrees of disintegration with bedding (where seen) at low angles of dip. Below this comes about 2 m of Head, which has been carried by the landslide from higher up the hillslope.

Borehole 10, located 320 m from the top, shows practically the full original ground profile (figures 12 and 13). A slip surface exists 10 cm above the base of 1.2 m of brecciated clay. At

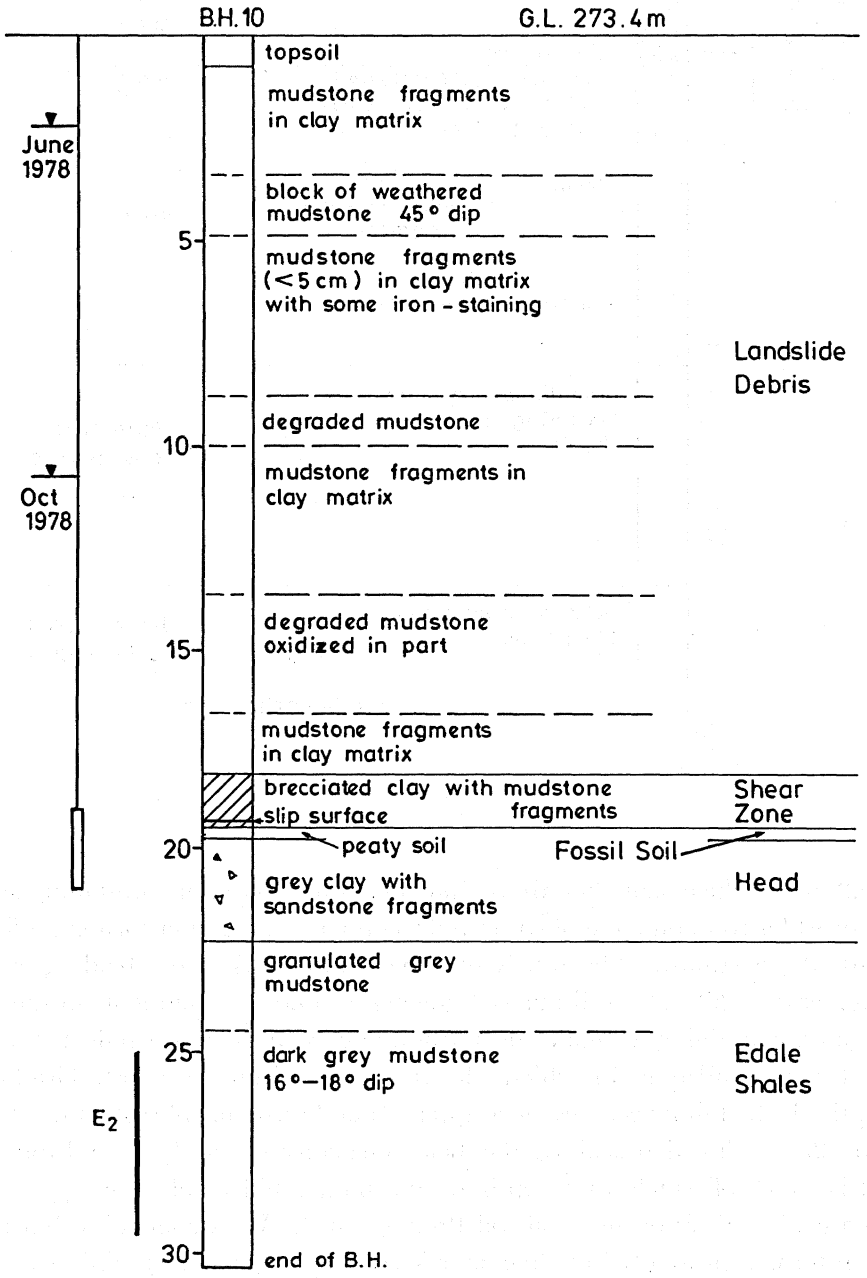

FIGURE 12

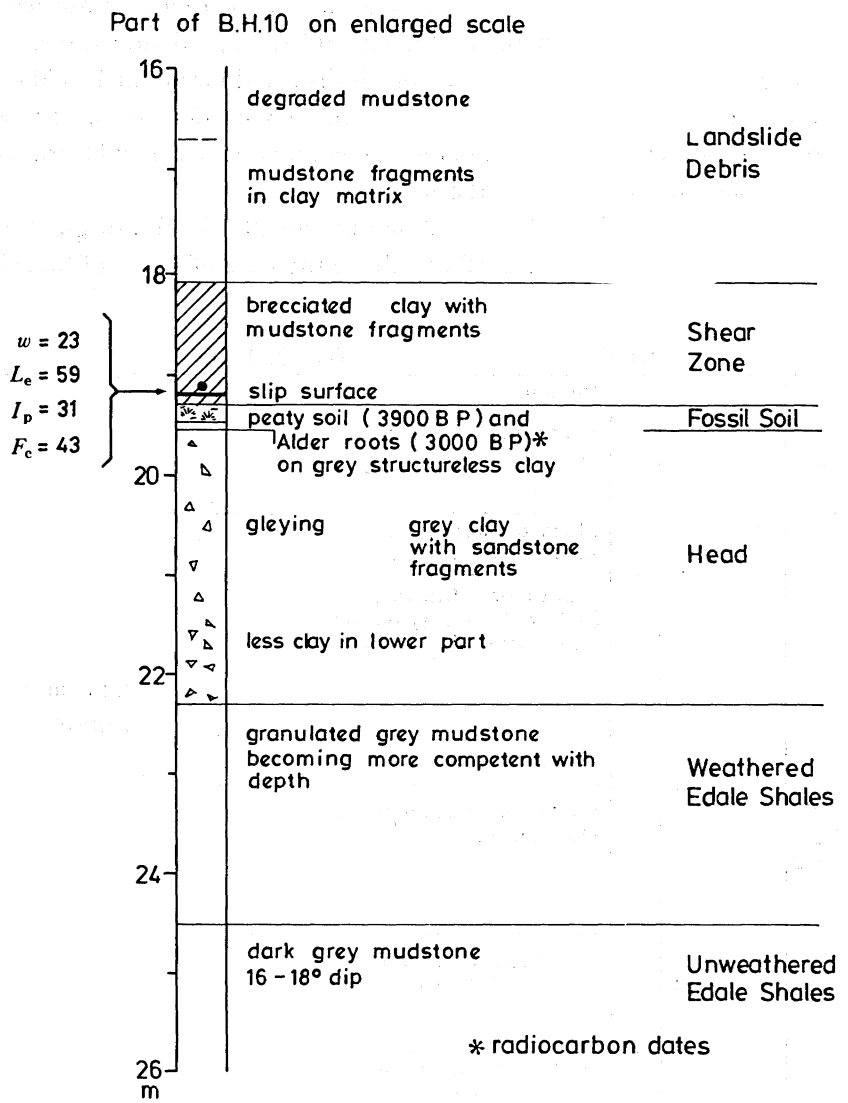

FIGURE 13

a depth of 19.3 m this shear zone lies above 15 cm of peaty material, containing small pieces of wood and an Alder root, on 5 cm of structureless grey clay; together forming a fossil topsoil buried beneath the earthflow. The soil is preserved above 2.7 m of Head; grey clay with sandstone fragments, exhibiting well-marked gleying around the fragments in the upper half of the deposit, and containing a smaller proportion of clay in the lower half. Below the Head is highly weathered mudstone in which all traces of bedding are lost. Gradually, with increasing depth, the bedding becomes more apparent and recognizable solid mudstone of zone E_2 is seen below 25 m. Slide debris above the shear zone consists mainly of mudstone fragments in a clay matrix, some of which, at a depth around 6 m, could be of zone R_{1a}.

From a botanical analysis of the fossil soil Professor R. G. West concludes that it is a local fen carr deposit formed probably in pollen zone VIIb (see Appendix 1). This is confirmed by

a radiocarbon date of 3900 years BP for the fine fraction. The Alder root yielded a younger date (as would be expected) of 3000 ± 150 radiocarbon years, in good agreement with the age of other wood fragments sieved out of the soil (Appendix 2). From correlations between radiocarbon and tree-ring dating (Pearson & Stuiver 1986) the absolute age of the Alder root is about 3200 ± 200 calendar years BP. Finally, analyses of samples from an auger hole near borehole 10 show that peat began forming in surface depressions at this locality some time after the beginning of pollen zone VIII; between 2500 and 2000 years BP (R. H. Johnson & J. H. Tallis, personal communication).

4. Landslide movements

About 3200 years ago an Alder tree growing in peaty soil at the location of borehole 10 was overwhelmed by the advancing earthflow. As this point is 320 m from the present toe of the landslide, movement has been taking place during this long period at an average rate of 10 m per century. However, the movements would occur not as continuous creep but rather as a series of small displacements in winter months of heavy rainfall, with correspondingly high piezometric levels. A quantitative understanding of the nature of this process can be gained from movements of the road, rainfall records and an analysis based on the response of groundwater level to winter rainstorms (§10).

The road across Mam Tor landslide was first built, by the Manchester and Sheffield Turnpike Trust, in 1810 to avoid an even steeper road in Winnats Pass, a limestone gorge 1 km to the south. Maintenance was doubtless required from time to time when slips occurred, and from 1907 brief notes of such work have been kept by Derbyshire County Council. A summary of the relevant information from 1915, when local rainfall records become available, is given in table 2. Movements usually arise from reactivation of the transition and earthflow sectors of the landslide, revealed by tension cracks in or above the 'upper' road, accompanied by subsidence and outward displacements; in some cases with upheaval on the edge of the slide (figure 7). More rarely almost the entire landslide is reactivated, as in December 1965. Slips of varying magnitude have been noted on 16 occasions during 66 years, on average at four-year intervals, and typically they are confined to December, January or February with monthly rainfall exceeding 200 mm.

One of the largest slips began on 10 December 1965 when cracks appeared following 120 mm of rain in six days (figure 14). Severe movements were noticed on 18, 23 and 29 December, in each case within a day of further rainy spells. By mid-January, when movement had practically ceased, the total displacement in the slump sector amounted to 0.7 m, as seen at point K in figure 1, and shear displacements of about 0.5 m were observed where the road crosses the flanks of the slide near points F and G (Brown 1966; R. D. Brown, personal communication). Most of this movement would have taken place during the last 20 days of December at an average rate around 30 mm day^{-1}. The upper road subsided by as much as 1.5 m in places and a local 'confined' slip developed over a short width below the road.

Observations, commenced on 20 January, of displacements at points I, F and G (R. D. Brown, personal communication) showed renewed activity in February, mainly in response to 100 mm of rain in 10 days towards the end of the month. The rate at that period was about

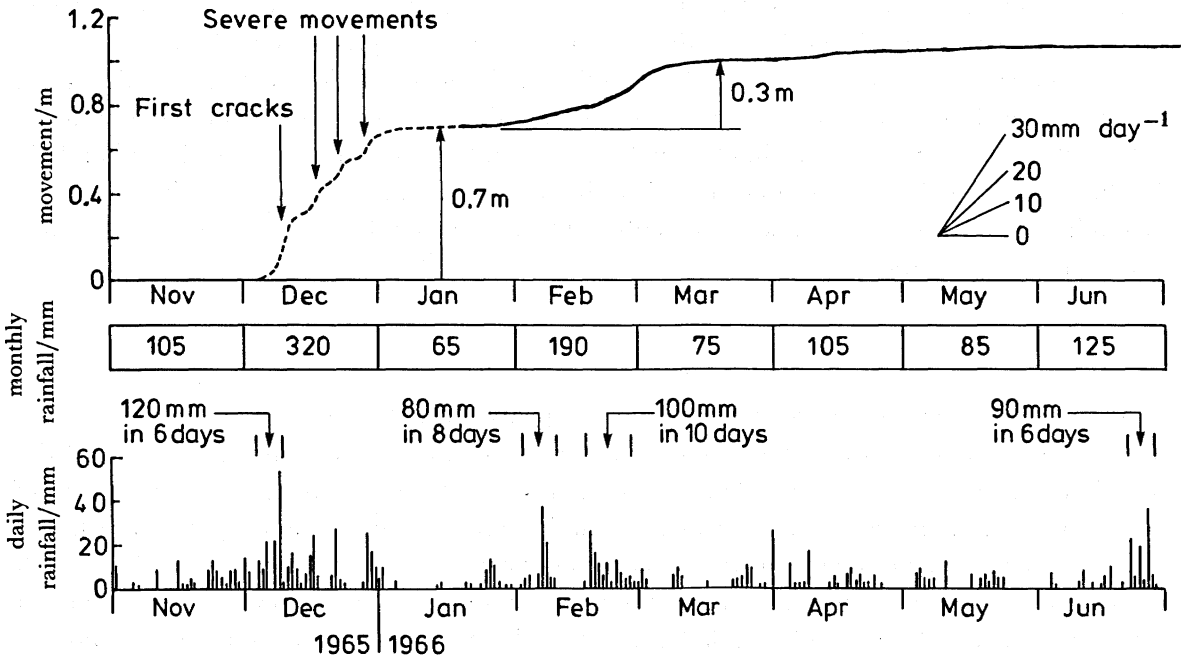

FIGURE 14. Rainfall and landslide movements, 1965–66.

15 mm day^{-1} and diminished almost to zero by mid-March (figure 14). The mean displacement at I and F, taken as representing the upper road, was 0.3 m between January and March. A further 0.04 m occurred in April but thereafter the slide remained stationary throughout the summer.

Movements of the lower road are consistently less than at the upper road, an observation consistent with the existence of compression ridges. Forward movements of the toe are therefore smaller than at the upper road, though on a long timescale the difference cannot be great, and clear proof of advance of the toe in recent times is provided by slide debris encroaching on Blacketlay barn (figure 10).

From observations in 1918, 1939, 1965, 1966 and 1977 the average displacement of the upper road when a reactivation slip occurs is about 0.3 m, allowing for the fact that not all slips involve the full width. With a return period of four years this is equivalent to 7.5 m century^{-1}, and because the toe of the landslide will have moved by a rather smaller amount the present rate of advance is evidently less than the average of 10 m century^{-1} for the past three millenia.

Interestingly, Bateman (1884) reports that a road crossing an earthflow within an ancient landslide on the north side of Rhodes Wood reservoir, in Longdendale, moved 3 ft in 13 years (7 m century^{-1}) though it had been stationary for some time before December 1850 when reactivated by engineering works. The earthflow, 80 m wide, extends about 300 m up a 12° slope in the Tintwistle Knarr landslide in Grindslow Shale of the middle Millstone Grit Series (Tallis & Johnson 1980) and Bateman notes that the slip surface was at a depth of 5.5 m. He also reports that an adjacent landslide (Didsbury Intake, about 20 hectares in area with an average slope of 11° below the scarp foot) moved 0.2 m in the night of 6–7 February 1852 after very heavy rain; doubtless further movements occurred subsequently. The rainfall, recorded

at Crowden Hall, 2.5 km to the east at about the same altitude (210 m OD) as the landslide, can be summarized as follows.

January 1852 = 127 mm (normal for this month)
February 1–3 = 36 mm
February 4–6 = 79 mm } 115 mm in 6 days
February 7–9 = 50 mm

This is then followed by a dry spell. Thus at Rhodes Wood, as at Mam Tor, a winter rainstorm of 115–120 mm in six days is capable of initiating substantial slip movements.

TABLE 2. RECORDS OF MOVEMENT AND RAINFALL

slip	date	movements	monthly rainfall/mm
1	January 1915	crack 30 m in length	200
2	December 1918	slip, 0.3 m subsidence	240
	January 1919	movements continue	140
3	December 1919	steady movement	280
	January 1920	movements continue	200
4	December 1929	serious slip	300
	January 1930	movements continue	180
5	January 1931	slip, 60 m crack	210
	February 1931	movements continue	190
6	February 1937	considerable subsidence	220
7	January 1939	100 m crack, 0.25 m subsidence	210
8	October 1942	30 m crack, 0.1 m subsidence	160
9	February 1946	extensive slip	240
10	November 1946	new movements	230
11	February 1948	subsidence on 200 m length (preceded by 280 mm rain in January)	100
12	December 1949	slip (no details)	230
13	January 1952	large slip (preceded by 400 mm rain in November and December)	150
14	December 1965	serious slip, 0.7 m displacement	320
15	February 1966	renewed movement, 0.3 m displacement (preceded by 385 mm rain in December and January)	190
16	February 1977	large slip; 0.4 m subsidence (average)	230

5. RAINFALL

Three rainfall stations in the vicinity of Mam Tor are listed in table 3. The records for Edale Mill and Mam Nick, the two nearest, are similar to each other with regard both to annual totals and variations on a monthly basis, and the rainfall at these stations can be taken as representative of the landslide. For early records, back to 1915, it is necessary to refer to Killhill

TABLE 3. RAINFALL STATIONS

location	grid reference SK43	distance from landslide/km	altitude/(m OD)	average annual rainfall/mm
Mam Nick	123837	1.0 W	417	1260
(centre of landslide)	133836	—	300	—
Edale Mill	134854	1.8 N	221	1250
Killhill Bridge	171838	3.8 E	171	1050

PHILOSOPHICAL TRANSACTIONS OF THE ROYAL SOCIETY A MATHEMATICAL, PHYSICAL & ENGINEERING SCIENCES

Bridge (near Hope), the monthly figures there being translated with sufficient accuracy by an increase of 20 % proportional to the annual rainfall. The average monthly rainfall, normalized to an annual total of 1250 mm, is given in figure 15*a*, while figure 15*b* shows the number of occasions from 1915 to 1980 inclusive in which rainfall exceeds 200 mm.

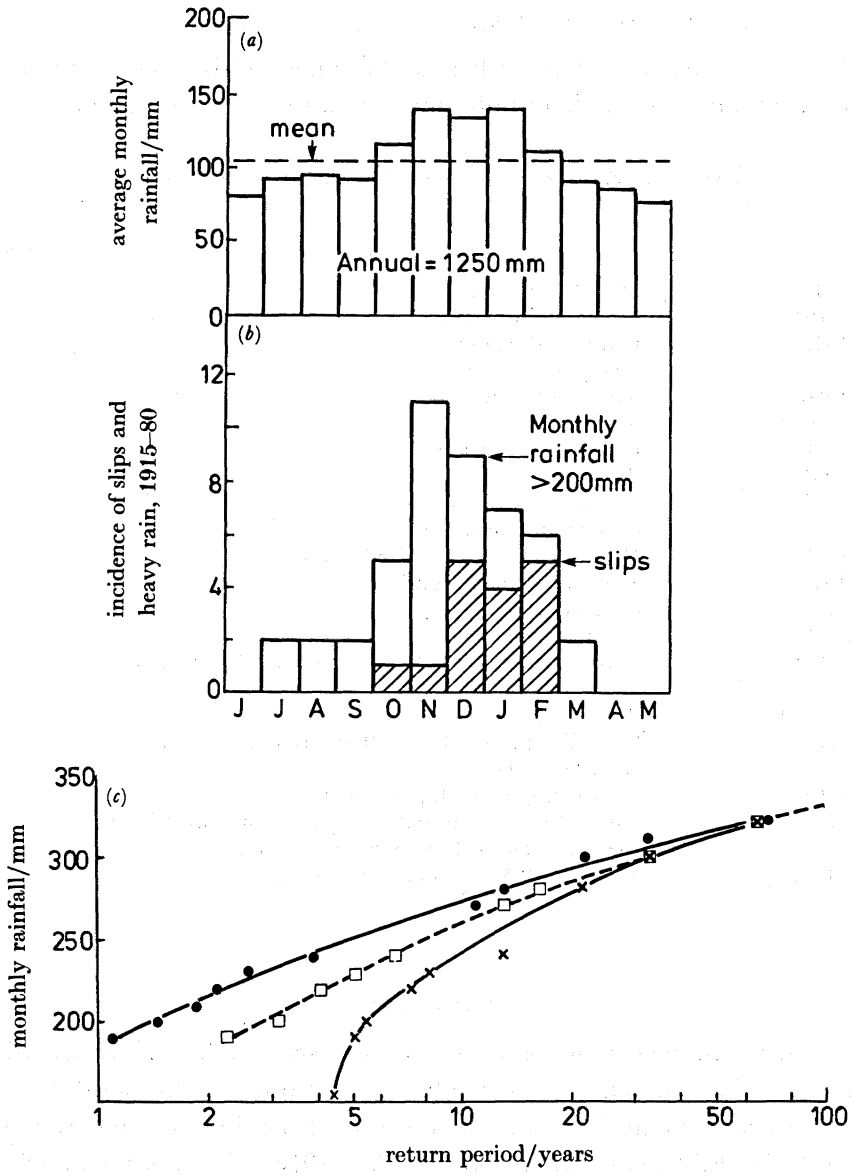

FIGURE 15. Rainfall and slips. ●, 12 months; □, December, January and February; ×, slips; (1915–80).

During this period 16 reactivation slips took place at Mam Tor. They are listed, with the relevant monthly rainfall, in table 2. Their frequency is shown in figure 15*b*. Twelve of the slips occur in winter months of heavy rainfall (greater than 200 mm), the distribution being: November (1), December (5), January (3) and February (3). Three other slips also occurred in January and February, but with average or moderately heavy rainfall; they follow, however, periods of very heavy rain. The small slip in October 1942 appears to be anomalous. With this

exception, the incidence of slipping follows a consistent pattern when related to the seasonal tendency for groundwater to rise (from its low summer and autumn levels) during November, December and January and to reach a maximum generally in February. Thus November has the largest number of monthly rainfalls exceeding 200 mm but only one slip; the proportion is much greater in December and January and reaches 80% in February. Conversely, heavy rain in other months (an extreme example being September 1918 with 300 mm) produces no instability.

An analysis of the records in terms of return period is plotted in figure 15*c* and the winter monthly figures are given in table 4 together with the rainfall for shorter durations, derived

TABLE 4. MAM TOR LANDSLIDE: RAINFALL STATISTICS AND PROBABILITY OF SLIPPING

(Annual average is 1250 mm.)

return period	winter rainfall/mm				probability of
years	3-day	6-day	10-day	1-month	slipping
2	50	70	90	180	0.4
3	55	80	105	200	0.5
5	65	90	120	230	0.6
10	75	105	135	260	0.7
20	85	115	150	285	0.85
50	100	130	165	310	1.0
100	110	145	180	330	1.0

from statistics in the Flood Studies Report (1975). For return periods of 20–50 years the monthly winter rainfall is about 300 mm and the six-day and 10-day values are around 120 mm and 160 mm respectively. These correspond closely to the records for Rhodes Wood in February 1852 and Mam Tor in December 1965, and a comparison between the return periods for winter rainfall and frequency of slipping at Mam Tor shows that instability there is almost certain to occur. Towards a lower limit when the monthly rainfall in December, January or February is 200 mm the 10-day rainfall will be around 100 mm, as was the case at Mam Tor in February 1966, and for every 10 such events about five may be expected to result in a slip; when no slip occurs winter groundwater will have been lower than its average level.

6. GROUNDWATER

(*a*) *Seasonal response*

Groundwater levels in the landslide are known from measurements taken by means of Casagrande-type piezometers (Casagrande 1949) carefully sealed in boreholes at a depth close to or within the shear zone (figures 8–12). Observations at about monthly intervals were continued for two comparatively short periods in 1977 and 1978, and have therefore to be assessed in relation to a general pattern of seasonal and short-term fluctuations.

Three groundwater records in clay slopes are plotted in figure 16 together with the monthly rainfall for (*a*) Barnsdale near Empingham in Leicestershire (R. J. Chandler, personal communication), (*b*) a small landslide on the north face of Bredon Hill in Worcestershire (Skempton & Henkel 1958) and (*c*) Uxbridge, 25 km northwest of London (Black *et al.* 1958). These, supplemented by a five-year record for Harmondsworth, a level site 27 km west of

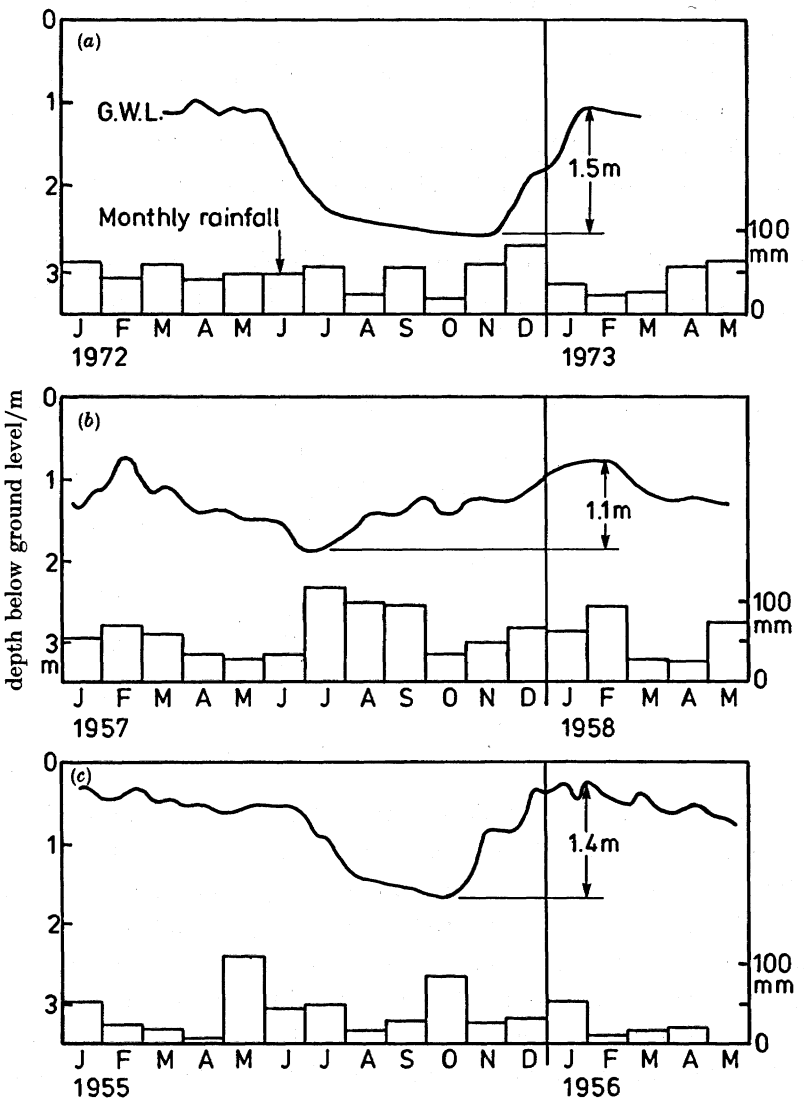

FIGURE 16. Seasonal fluctuation in groundwater level. (*a*) Barnsdale, Upper Lias, 7° slope, piezometer at 3 m. (*b*) Bredon Hill, Middle Lias, 12° slope, piezometer at 2 m. (*c*) Uxbridge, London Clay, 4° slope, covered borehole.

London (Black *et al.* 1958) show that groundwater is normally at its lowest level in October, following the summer depletion, and rises to its highest level in January or February, following the winter recharge.

Two or three months of abnormal rainfall can distort the pattern, but the maximum and minimum levels are not greatly affected. Thus in the Harmondsworth record, January–February groundwater in two wet winters (rainfall 30% above average) was 0.25 m above the level for average winter rain. This particular observation is not influenced by rainstorms. Their effect is considered in §§6(*b*) and 10; here it may be remarked that short spells of heavy rain or dry weather can commonly cause a temporary rise or fall in groundwater level of about 0.2 m. Consequently, readings taken at monthly intervals, as at Mam Tor, can define a seasonal maximum or minimum only within this limit of accuracy.

Observations in boreholes 1 and 7 are plotted in figure 17, with rainfall as measured at Mam

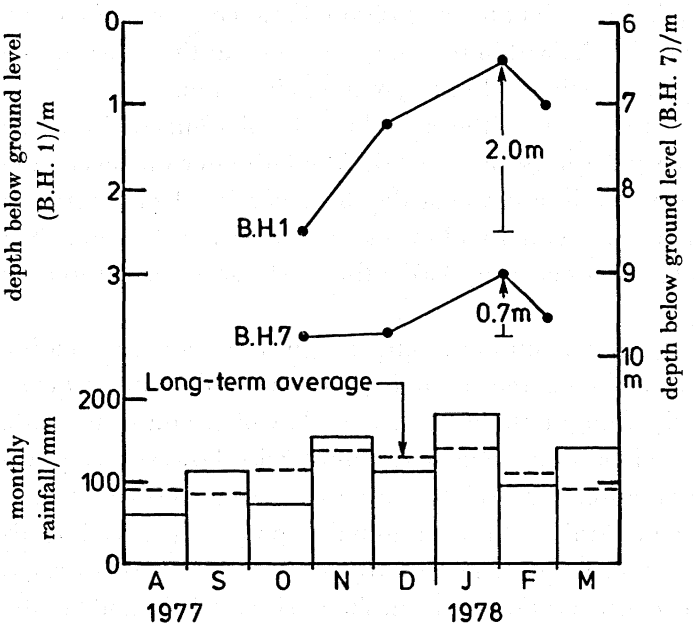

FIGURE 17. Piezometric levels, Mam Tor landslide.

Nick. The first readings, towards the end of October 1977, follow a spell of moderate rain in a rather dry month, preceded by unexceptional rain in September and August. The late-October groundwater is therefore probably close to its normal minimum level. By contrast, the readings in early February 1978 are at, or even a little above, the normal maximum level; they were taken after a wet January (185 mm) following approximately average rainfall in the two preceding months.

Borehole 7, in the slump section of the landslide, shows a seasonal response of 0.7 m; much the same as in the similarly situated borehole 6. At borehole 1, in the upper part of the earthflow, the response is 2.0 m. Vandalism of the installations prevented further readings after a small drop in level during the later part of February. Borehole 2 was lost in December; it showed a rise of 0.5 m before being destroyed. The piezometer in borehole 4 was accidentally damaged during installation. Water levels in the ponds were accurately surveyed in February 1978.

The piezometers in boreholes 8, 9 and 10 were first read in mid-June 1978 after moderately heavy rain following two months of less than average rainfall. Groundwater at this time would therefore be lower than the maximum levels. In borehole 8, in the slump sector, water was 8.7 m below ground surface. It dropped to 9.1 m by October–November, in unexceptional conditions, probably to about the normal minimum. By analogy with the nearby boreholes 6 and 7 the maximum level in February 1978 would thus have been at a depth of about 8.4 m below ground.

The piezometer in borehole 9, adjacent to borehole 4, was installed on 6 June 1978 in weathered mudstone beneath the slide debris (figure 9). From mid-June to mid-July piezometric level rose by a small amount, indicating a slow rate of equilibration and a correspondingly low permeability. Thereafter it remained practically constant, the level in October (before the piezometer was destroyed) being 9.9 m below ground. As borehole 9, in

PHILOSOPHICAL TRANSACTIONS OF THE ROYAL SOCIETY A MATHEMATICAL, PHYSICAL & ENGINEERING SCIENCES

the transition sector, is intermediate in position between boreholes 6 and 1 the seasonal response may be assumed to lie within the range recorded at these locations, giving a probable depth to maximum piezometric level of approximately 8.6 m.

At borehole 10, near the centre of the earthflow, the piezometer (in the shear zone) showed in mid-June a water level 2.2 m below ground. A month later the level had dropped to 6.5 m and by October–November it stood at a depth of nearly 11 m. Moreover, when the next reading was taken, after a wet winter and spring (850 mm since the end of November, of which, 470 mm fell in March, April and May 1979) the level had returned to a depth of 3 m below ground.

A seasonal range of this magnitude is surprisingly large for the conditions at Mam Tor, suggesting that the winter recharge, though partly derived from vertical infiltration in the usual manner, is chiefly brought about by throughflow of groundwater within the slide debris from higher parts of the landslide. Some doubt must exist, however, concerning the validity of these particular observations; especially because piezometers in a broadly comparable earthflow, in the Blaina landslide, show a seasonal response not exceeding about 2 m (Jones & Siddle 1988). Nevertheless, large variations are on record. A seasonal response ranging from 3 to 8 m over 10 years of observation occur in slide debris (Chalk and Gault clay) near the toe of the large Folkestone Warren landslide in Kent (Hutchinson 1969) and the effect of throughflow is well documented in Hong Kong. There, towards the foot of high and steep (greater than 20°) slopes, piezometers at depths of 20–30 m in completely weathered granite soil, having the properties of a dense silty sand (permeability equals 7×10^{-6} m s^{-1}), show a response up to 10 m during the wet season: typically with 1200 mm of rain in five months (Insley & McNicholl 1982).

The maximum piezometric level in borehole 10 can be found with sufficient accuracy for practical purposes by graphical interpolation between the known elevations of water in February 1978 at boreholes 1 and the pond, making use also of the more remote borehole 9. It is about 1.8 m below ground, allowing for 0.3 m difference from groundwater level.

A summary of data on the line of section is set out in table 5. As mentioned earlier, the elevations of water in February 1978 may be taken as representing the piezometric level in the shear zone at a time when groundwater is close to its seasonal maximum under normal conditions.

(*b*) *Storm response*

Knowledge of the groundwater response, in clay soils, to spells of heavy rain can be gained from an examination of cases where weekly readings are available over a sufficient period of time to include one or more rainstorms. An example from the Uxbridge site is shown in figure 18. Minor oscillations in October and November are followed by a rise of 0.3 m caused by 70 mm of rain falling in eight consecutive days. Apart from a small interruption by a single day of heavy rain, the water table then falls during a dry spell and is restored to its winter level in January.

In winter months, when negative pore pressures (suction) and soil moisture deficit are effectively zero the greater part of the rainfall not 'lost' as run-off is able to seep down to the water table without being absorbed by the soil. Under such conditions the 'storm response' in groundwater level Δh is to a first approximation directly proportional to the rainfall R (see figure 19), and the ratio $\Delta h/R$, equal to about 4.0 in the example in figure 18, may be taken as a characteristic parameter for any particular site.

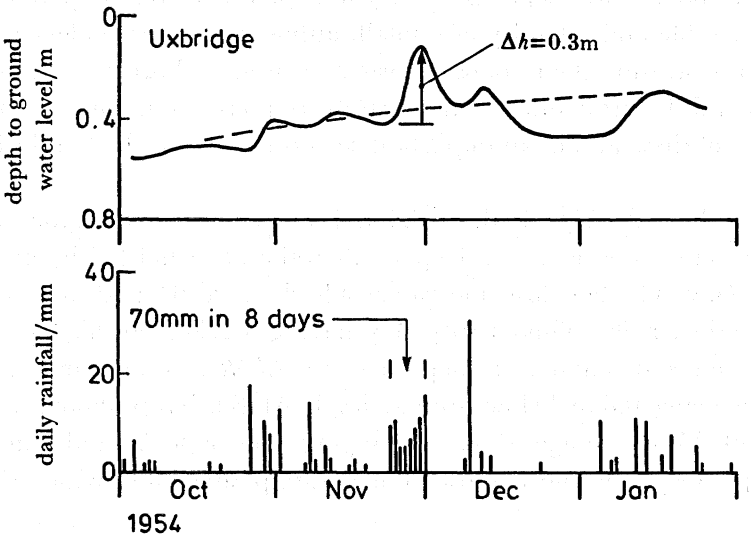

FIGURE 18. Groundwater response to fluctuations in rainfall.

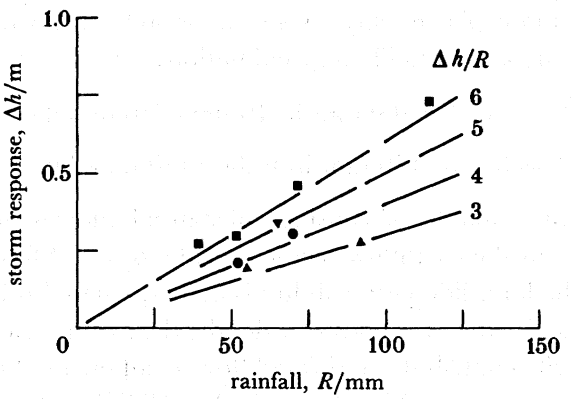

FIGURE 19. Winter storm response and rainfall. ■, Harmondsworth; ●, Uxbridge; ▲, Burderop Wood; ▼, Bredon Hill. Rain intensity is 5–10 mm day^{-1}.

TABLE 5. PIEZOMETRIC LEVELS

borehole	ground surface/(m OD)	distance from toe of landslide/m	seasonal response/m	piezometric level February 1978 depth below ground/m	probable error/m	elevation /(m OD)
8	359.8	700	0.7	8.4	±0.2	351.4[c]
9[a]	309.6	520	1.3	8.6	±0.5	301.0[c]
1	280.2	390	2.0	0.5	0	279.7[b]
10	273.3	320	9(?)	1.8	±0.5	271.8[c]
pond	—	230	—	—	+0.3	265.4[b]

[a] Adjacent to borehole 4.
[b] Measured.
[c] Estimated, with probable error as noted.

The winter storm-response ratio depends upon several factors including permeability, slope angle, depth to water table and intensity of rainfall, although there is evidence (Bertini *et al.* 1984) that in a uniform stratum the response, seasonal as well as short term, is practically the same in piezometers at different depths. Data on storm-response from four sites are plotted in figure 19; a summary of these and of an important record from San Martino in Italy is given in Appendix 3.

At Harmondsworth the ratio $\Delta h/R$ is about 6.5 and may be near to an upper limit in clays, for although winter groundwater is rather deep at 2.6 m the site is flat (with minimal run-off) and the soil is sandy clay. The San Martino valley side slopes at 9°, and to a depth of 20 m, including a fissured crust, is in colluvial silty clay having a relatively high permeability of 5×10^{-7} m s^{-1}. Piezometers at 5 and 15 m depth showed $\Delta h/R$ ratios around 5.5, the winter water table typically being 0.6 m below ground level. At Burderop Wood, Uxbridge and Bredon Hill values of $\Delta h/R$ average about 4 (ranging from 3 to 5) and can be taken as representative of slopes in plastic clays of low to moderate permeability with a shallow water table.

In the earthflow sector of Mam Tor landslide $\Delta h/R$, for the same intensity of rainfall, will be somewhat less than at San Martino, where conditions are similar except that the shear zone is probably less permeable than the silty clay. Conversely, $\Delta h/R$ in the earthflow is likely to be greater than in slopes of more plastic clay. A storm response ratio between 4 and 5 may therefore be considered to be a reasonable approximation; say

$$\Delta h/R = 4.5 \quad \text{for 100 mm in 10 days (10 mm day}^{-1}\text{)}$$

increasing to

$$\Delta h/R = 5 \quad \text{for 120 mm in 6 days (20 mm day}^{-1}\text{)}.$$

Thus for winter rainstorms capable of causing substantial movements the corresponding transient groundwater rise in the earthflow sector is of the order of 0.5 m.

In the slump sector of the landslide permeability is higher, where broken sandstone exists in the debris, but winter groundwater is at a greater depth; the average slope is steeper, but run-off from the scarp face will contribute a throughflow component. On balance it may be concluded that the storm response in this part of the landslide is not very different from that in the earthflow, and in any case is unlikely, even as an upper limit, to exceed the seasonal response of 0.7 m measured in borehole 7.

(*c*) *Chemistry*

Oxidation of pyrite (FeS_2) within the mudstone results in the release of sulphuric acid, which liberates iron, calcium and other elements into solution. Chemical analysis shows the process to be operative in the Mam Tor landslide (Vear & Curtis 1981) because water issuing from

TABLE 6. GROUNDWATER CHEMISTRY

water		pH	ion concentration/(mg l^{-1}) Al	Ca	K	Fe	SO_4
from earthflow	springs	3.1	13	220	6	60	820
	seepage	3.1	4	170	7	35	610
surface run-off		5.2	0	20	2	3	100

springs and seeping off the earthflow in winter is acidic with an ion concentration much in excess of that in run-off from adjacent slopes, for example in the stream near Blacketlay Farm: see table 6.

Exploratory tests related to the failure of Carsington dam, south Derbyshire (Babtie Shaw and Morton & Skempton 1986), show, however, that the effect of complete leaching with sulphuric acid is to reduce the peak shear strength of fresh (unoxidized) compacted pyritic Edale Shale by only about 7 %, at the stress levels appropriate to Mam Tor landslide, and there are indications that the reduction in residual strength is even less. Consequently, the contribution of these chemical reactions to the continued movements of the slide debris is likely to be small. Strength and other properties determined in the present investigation are those obtaining after at least 3000 years of landslide activity.

7. Index properties

Water content, liquid limit (L_l) and plastic limit (L_p) were measured in specimens cut from 100 mm diameter cores of slide debris, taken in boreholes 1 and 2, and of shear zone material in boreholes 1, 2 and 10. Average values of these index properties are given in table 7. Plasticity index ($I_p = L_l - L_p$) for individual tests is plotted against liquid limit in figure 20. Most of the clay matrix samples giving points close to the A-line of Casagrande (1947) can be classified as clays of medium plasticity. Their water contents are on average 3 percentage points lower than the plastic limit, typifying a stiff overconsolidated clay. On the plasticity chart the mudstone cannot be distinguished from the matrix, but its water content is considerably lower. Standard

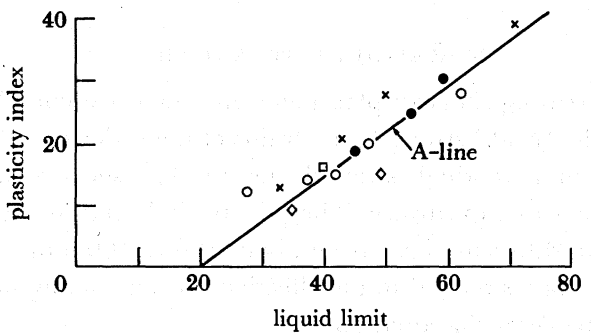

Figure 20. Plasticity chart for slide debris and shear zone. ○, Clay matrix; ◇, clay matrix (micaceous); □, mudstone; ●, shear zone; ×, Head.

Table 7. Index properties of slide debris and shear zone

material	boreholes	water content (w)	liquid limit (L_l)	plastic limit (L_p)	plasticity index (I_p)	clay fraction (F_c)
clay matrix	1, 2	22	43	25	18	—
clay matrix, micaceous	1, 2	23	42	30	12	—
mudstone	1	14	40	24	16	—
head	1, 2	21	49	24	25	—
slide debris, weighted mean	—	21	44	25	19	—
shear zone	1, 2, 10	22	53	28	25	35

penetration tests on the mudstone in borehole 1 give values of N in the region of 30, indicating that it has the strength of a very stiff to hard clay (Terzaghi & Peck 1948). Two micaceous clays fall, as usual, a little below the A-line. The three shear zone samples tend to have a higher plasticity than the clay matrix, whereas all four samples of Head, the most highly weathered material in the landslide, lie above the A-line with water contents (relative to the plastic limit) much like those of the clay matrix.

Particle-size analysis of the shear-zone material shows a clay fraction (F_c = percentage by mass of particles smaller than 0.002 mm) related to plasticity index by the ratio

$$I_p/F_c = 0.7$$

defined as the colloidal activity (Skempton 1953). This is similar to the activity of Edale Shales mudstone at Carsington (see table 8). It is also compatible with the clay mineralogy determined by Steward & Cripps (1983) on a sample of the mudstone, probably in zone E_2, from Hope Cement Works near Castleton:

Mixed layer	expandable component	50
	illite	21
Kaolinite		23
Chlorite		6
		100

The average water content from 19 samples of slide debris is about 21 % of the dry mass. For a specific gravity of the particles of 2.7 the corresponding unit weight of the material, assuming full saturation, is $\gamma = 20$ kN m^{-3} with a porosity of 36 %.

8. Residual strength

When subjected to increasing shear displacement an intact overconsolidated clay develops a maximum resistance, the 'peak' strength, at strains of the order of 10 % and thereafter the resistance falls to a minimum 'residual' strength (figure 21) associated with the development of a polished, striated shear or slip surface. The post-peak displacement required for the full drop in strength varies, in different clays, from about 100 to 500 mm.

The peak strength of a clay is related to the effective pressure acting normal to the plane of shearing by the Coulomb–Terzaghi equation

$$s = c' + (\sigma_n - u)\tan\phi', \tag{1}$$

where c' is the apparent cohesion, ϕ' is the angle of shearing resistance, σ_n is the total normal pressure, u is the pore water pressure and $(\sigma_n - u) = \sigma'_n$ is the effective normal pressure.

To a close approximation the relation between s and σ'_n is linear for most clays, as shown in figure 21. The post-peak drop in strength takes place essentially in two stages. First, a decrease in cohesion, with little change in ϕ', to the 'critical state' in which $c' = 0$; and second, a decrease in ϕ' to the residual value ϕ'_r. This second stage of the process results chiefly from reorientation of platy clay particles in the direction of shearing. As the relation between residual strength s_r and effective normal pressure is in general slightly nonlinear, the value of ϕ'_r, as defined by the expression $\tan\phi'_r = s_r/\sigma'_n$, is quoted in terms of a given value of σ'_n.

Before a slip occurs for the first time in a clay slope, the strength will usually be somewhat

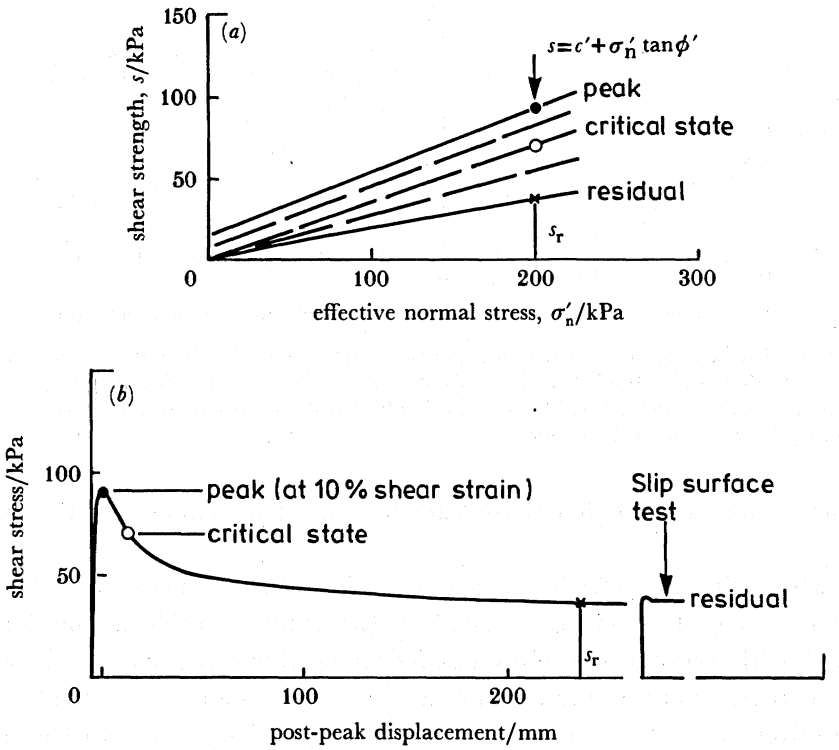

FIGURE 21. Shear strength and stress–strain relations for an overconsolidated clay. (*a*) $\phi'_r = \arctan(s_r/\sigma'_n)$. (*b*) $\sigma'_n = 200$ kPa.

less than the peak value because of the effect of creep or progressive failure resulting from non-uniform strain along the potential slip surface. But once the slip has started moving the strength begins to fall towards the much lower residual value, and movements continue, quite rapidly, and with large displacements, until a new position is reached with the slip mass in equilibrium with the residual strength. Subsequent movements may take place, due to disintegration of the slipped mass and repeated heavy rainfall, but the strength on a slip surface will remain at the residual value. Consequently, if a sample is taken and tested in such a way that failure occurs on a pre-existing slip surface, the strength measured in the test should be equal to the residual; and experience has shown that good agreement (with an error not exceeding 1° in ϕ'_r) is obtained between such 'slip surface tests' and the values of ϕ'_r calculated by back-analysis of reactivated landslides (Skempton 1985).

Tests of this kind are not easily carried out, and to obtain reliable results they must be made on at least three separate and virtually identical specimens, each tested under a different normal pressure. Data from such tests and in a few cases from modified procedures (Appendix 4) are plotted in figure 22 against both plasticity index and clay fraction, the values of ϕ'_r being taken at $\sigma'_n = 200$ kPa as appropriate for Mam Tor landslide (see table 9). The lines drawn in this figure are mutually consistent for an activity ratio (I_p/F_c) of 0.65; they may be considered as reliable correlations between ϕ'_r and the index properties for clays of this type. Clays of low plasticity are controlled to a great extent by the sand particles, and the nature of the clay fraction is practically irrelevant. With high clay fractions, however, clays of low activity tend to show larger values of ϕ'_r as a result of the dominance of kaolinite, while the dominance of

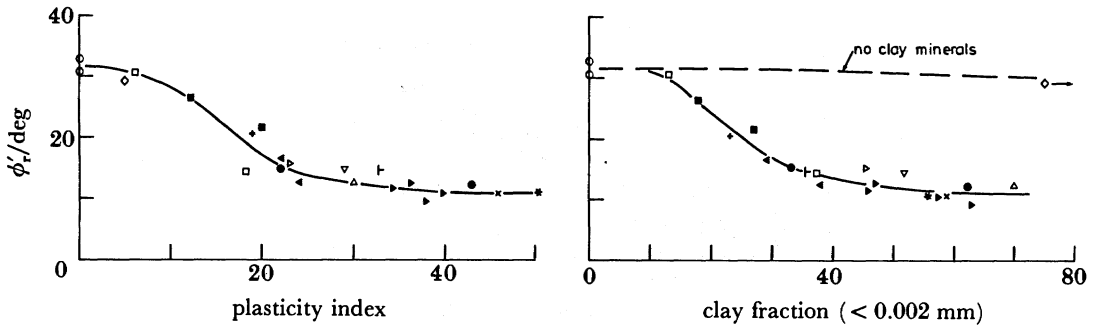

FIGURE 22. Correlation of field residual strength with plasticity index and clay function (values of ϕ'_r at σ'_n = 200 kPa). I_p/F_c = 0.4–0.6: △, Walton's Wood; ▷, Monmouth; ▽, Bury Hill; □, Kalabagh. I_p/F_c = 0.6–0.75: ▶, Jari; ■, Kalabagh; ●, Carsington; ◀, Mangla. I_p/F_c = 0.75–1.0: ×, Sevenoaks; +, Jari; ⊢, S. Barbara; *, London clay. ○, Sand; ◇, amorphous silica.

mixed layer minerals in clays of high activity leads to somewhat smaller ϕ'_r values, for a given clay traction.

At Mam Tor, where slip surface testing was not feasible, estimates of ϕ'_r can be obtained from the index properties: see table 8. The ϕ'_r value of 14–15° deduced in this manner for the shear zone compares well with test results on slip surfaces developed in compacted mudstone, having similar index properties, from the Edale Shales at Carsington dam (see Appendix 4). In the clayey slide debris from boreholes 1 and 2, with an average plasticity index of 19, ϕ'_r is probably about 18–19°, whereas on slip surfaces passing through sandstone debris, and in the scree, ϕ'_r for these non-plastic materials will be around 30°.

TABLE 8. MATERIALS DERIVED FROM THE EDALE SHALES

location	material	L_l	I_p	F_c	I_p/F_c	ϕ'_r at σ'_n = 200 kPa	
Mam Tor: transition and earthflow sectors	slide debris	44	19	—	—	18–19°	from figure 22
	shear zone	53	25	35	0.7	14–15°	
Carsington, Derbyshire	compacted mudstone fill	45	22	34	0.65	15°	slip surface tests
Atlow, Derbyshire	completely weathered mudstone	54	23				

All the residual strengths in figure 22 are derived from tests carried out at a slow rate of displacement; typically 5 mm day^{-1}. The results are not more than about 2% above the 'static' strength at virtually zero rate of displacement; see §10.

9. STABILITY ANALYSIS

The factor of safety of an actual or potential slip is defined as

$$F = \sum S / \sum T,$$

where $\sum S$ and $\sum T$ are respectively the sums of the shear resistance and the shear forces acting on the slip surface. For limiting equilibrium, when movement is about to take place, $F = 1.0$. If on any element of the slip surface the total normal stress is σ'_n and the shear stress is τ, then

$$F = \sum c' l + \sum (\sigma_n - u)\, l \tan \phi' / \sum \tau l, \qquad (2)$$

where c', ϕ' and u are defined by equation (1) and l is the length of slip surface in the element.

When the total length of a slip is large in relation to its depth, as at Mam Tor, F can be evaluated with little loss of accuracy in the two-dimensional case by dividing the mass into a number of vertical-sided slices (figure 23) and taking

$$F = [\sum c' l + \sum (W \cos\alpha - ul) \tan\phi'] / \sum W \sin\alpha, \tag{3}$$

where W is the mass of slice and α is the inclination of its base.

In (3) the tacit assumption is made that the effect of forces acting on the sides of the slices can be neglected. A more exact method, in which these forces are taken into account and conditions of internal equilibrium are satisfied (Sarma 1973), when applied to case 1 of the Mam Tor analysis (see below) gives a factor of safety 2.3% higher than the result obtained from (3).

In the actual three-dimensional slip the average shear force on the base of a slice is reduced by 'drag' on the outer edges of the slip mass. If the depth of slip at its edge is D, and the shear strength on the base is s, the drag force on each side will be approximately $\frac{1}{2}DKs$, where K is the coefficient of lateral earth pressure. The basal shear force is therefore reduced from the two-dimensional value (with $B = \infty$) in the ratio

$$1/(1 + KD/B). \tag{4}$$

The lateral pressure acting on the side of a landslide will be somewhat less than the 'earth pressure at rest', and K is likely to lie within the range 0.5–1.0. The upper limit of $K = 1.0$ may be taken to compensate for the neglect of internal forces, and (3) is then rewritten in its three-dimensional form:

$$F = [\sum c' l + \sum (W \cos\alpha - ul) \tan\phi'] / \sum W(1 + D/B)^{-1} \sin\alpha. \tag{5}$$

Four cases are examined by using (5), with W calculated from a unit weight of 20 kN m^{-3} and taking

$$u = \gamma_w h, \tag{6}$$

where γ_w is unit weight of water (9.8 kN m^{-3}) and h is the piezometric height above the slip surface to winter groundwater, as observed (or deduced) in February 1978. Under this condition the landslide is close to limiting equilibrium, with $F = 1.0$, because it can be substantially reactivated by a transient rise in water level of 0.5 m (see §6). Moreover, because large displacements have occurred in the past, the strength along a slip surface must be at the residual, with $c' = 0$ and a 'static' angle of shearing resistance ϕ'_r.

Case 1. Reactivation of the landslide frequently involves tension cracks at the upper road, point j in figure 23, and sliding on a slip surface passing through slide debris and along the basal shear zone. The values of ϕ'_r for these materials, as given in table 8, lead to factors of safety within 10% of the correct value ($F = 1.0$), the best result being obtained with $\phi'_r = 14°$ (shear zone) and $\phi'_r = 18°$ (slide debris), when the calculated value of F is 1.02.

Case 2. As a variant of case 1 the slip surface is assumed to thrust upward through the slide debris at point k. This simulates a 'confined' slip not extending to the toe of the earthflow. With the same residual parameters $F = 1.00$, confirming that these two modes of failure have very similar probabilities.

Case 3. In the slip of February 1977 cracks were seen above the upper road, as at point h in figure 23, additionally to those at the road. On the slip surface hd a higher value of ϕ'_r may be taken because the slide debris here probably includes a considerable proportion of sandstone, as observed in nearby borehole 6. A reasonable assumption is that about one-third of the debris

PHILOSOPHICAL TRANSACTIONS OF THE ROYAL SOCIETY A MATHEMATICAL, PHYSICAL & ENGINEERING SCIENCES

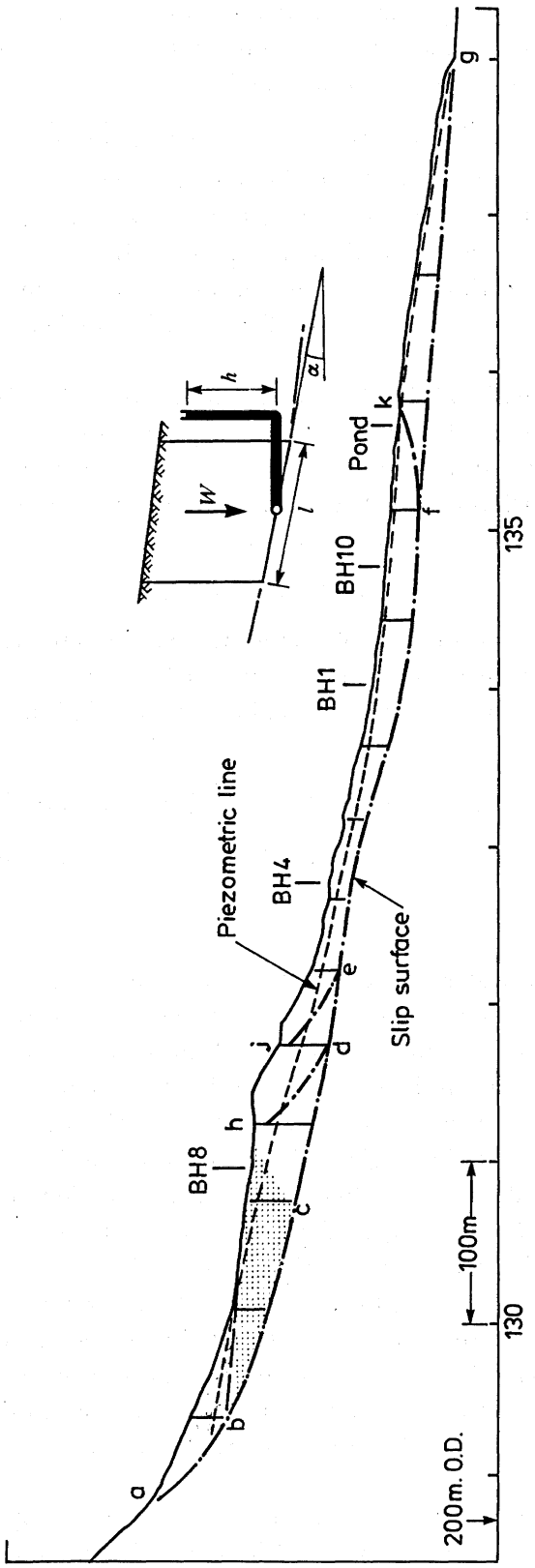

FIGURE 23. Stability analysis.

PHILOSOPHICAL TRANSACTIONS OF THE ROYAL SOCIETY A MATHEMATICAL, PHYSICAL & ENGINEERING SCIENCES

is sandstone, with $\phi'_r = 30°$, and the rest is clayey debris with $\phi' = 18°$. The average residual angle on hd is then 22° and, still using $\phi'_r = 14°$ in the basal shear zone, $F = 0.99$. Had it been assumed, as perhaps an upper limit, that half of the debris consisted of sandstone the average value of ϕ'_r on hd would be 24° and the corresponding factor of safety is increased by 1.7% to $F = 1.02$.

Case 4. Exceptionally heavy rain in December 1965 led to reactivation of practically the entire landslide up to and including the scree. The scree is granular material with little if any clay fraction, in which ϕ'_r can be taken as 30° (figure 22). The shear zone bc (figure 23) will contain a rather high proportion of sand, derived from the overlying predominantly sandstone debris in this upper part of the slump. Reference to figure 22 shows that ϕ'_r in sandy clays is very dependent on relatively small changes in plasticity index and clay fraction. The procedure in this case must therefore be to determine by back-analysis a value of ϕ'_r in the shear zone bc which gives a factor of safety not less than 1.0, with $\phi'_r = 14°$ in the slip below point c. The result is a value of ϕ'_r lying between 23°, which gives $F = 1.0$ exactly, and 24° leading to $F = 1.02$.

From figure 22 a value of $\phi'_r = 24°$ corresponds to a clay fraction of approximately 20%; an acceptable result, as compared to 35% in the shear zone further down the landslide where the debris consists chiefly or entirely of degraded mudstone and clay matrix.

Thus it will be seen from these four cases that no difficulty exists in showing that the landslide as a whole and various parts of the landslide are delicately balanced in a state close to limiting equilibrium with groundwater level (GWL) at about the normal winter maximum. A summary of the analyses is given in table 9.

It remains to examine the effect of variations in the parameters and assumptions used in the analysis; see table 10. An increase in ϕ'_r in the basal shear zone from 14 to 15° leads to an

TABLE 9. STABILITY ANALYSIS

case	slip surface	ϕ'_r/deg	GWL as in February 1978 σ'_n/kPa	F	reduction in F due to $\Delta h = 0.5$ m (%)
4	a–b	30	140	1.02	2.0
	b–c	24	220		
	c–g	14	210		
3	h–d	22	210	0.99	2.6
	d–g	14	180		
1	j–e	18	170	1.02	2.9
	e–g	14	170		
2	j–e	18	170	1.00	2.9
	e–f	14	190		
	f–k	18	120		

TABLE 10. CHANGE IN FACTOR OF SAFETY (PERCENT)

case	increase in ϕ'_r from 14 to 15°	effect of internal forces	decrease in K from 1.0 to $K = 0.5$	to $K = 0$	piezometric level increased by 0.5 m
4	+5.1	—	−4.3	−8.6	−2.0
3	+6.4	—	−2.5	−5.1	−2.6
1	+6.7	+2.3	−2.0	−4.0	−2.9
2	+5.3	—	−2.2	−4.5	−2.9

increase in F by 5–7 %, and a reduction to 13° would produce a similar decrease in F. Changes of this magnitude are not admissible and indicate that $\phi'_r = 14°$ is the correct value within narrow limits. If the lateral earth pressure coefficient K is taken as 0.5, instead of 1.0, F is reduced by 2–4 %. Conversely, if internal forces are taken into account F (in case 1) is increased by 2.3 %. As previously mentioned, $K = 1.0$ may be near an upper limit and as such has been adopted in order approximately to counteract the neglect of internal forces in equation (5). It may be noted in passing that if the three-dimensional effect is ignored altogether (by putting $K = 0$) a more serious error is involved, possibly amounting to at least 4 % in case 4. Finally, a change in groundwater level of 0.5 m results in a change in factor of safety of 2–3 %. This can be regarded from two points of view. (i) As an uncertainty in the piezometric head h in (6) it leads to a variation up to 3 % in the value of ϕ'_r required for $F = 1.0$; a minor effect expressed for example by $\phi'_r = 14 \pm 0.4°$ in the basal shear zone. But (ii) when considered as a rise in groundwater level the effect is to reduce the factor of safety by 3 % and, as shown in the following section, this is sufficient to cause substantial reactivation of a landslide previously existing in a state of limiting equilibrium.

10. Mechanics of storm-response movements

Storm-response movement may be defined as the displacement caused by a transient rise in piezometric level $\Delta h'$ above the level corresponding to a state of limiting equilibrium ($F = 1.0$) with the static residual strength. A piezometric rise δh will cause an increase in pore pressure in the shear zone $\delta u = \gamma_w \delta h$ and therefore a decrease in shear strength, according to equation (1). Consequently, the factor of safety falls below 1.0 and movement will occur. However, in clays of medium to high plasticity the shear strength increases with rate of displacement, as shown in figure 24. Movement is therefore restricted to a finite amount.

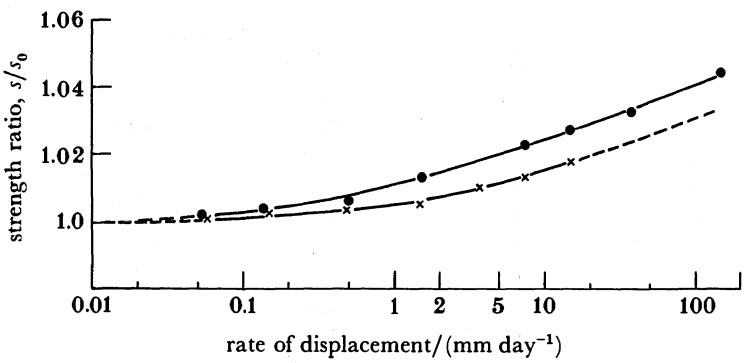

Figure 24. Relation between residual strength and rate of displacement. ●, London clay ($L_1 = 82$, $I_p = 49$); ×, weathered Edale Shale ($L_1 = 54$, $I_p = 23$).

The rates of movement involved are sufficiently low (of the order of 100 mm day^{-1}) for inertial forces to be negligible. If, then, a piezometric rise δh causes a drop in factor of safety δF the rate of displacement $\dot{x}$ will be such as to give a strength increase,

$$s/s_0 = (1 + \delta F)/1, \tag{7}$$

where s_0 is the static strength corresponding to $F = 1.0$. If this piezometric head acts for a time δt, the incremental displacement $\delta x = \dot{x}\,\delta t$, and the total displacement will be

$$\Delta x = \sum \dot{x}\,\delta t. \tag{8}$$

As an example, consider the response curve sketched in figure 25 for a six-day rainstorm. Assume that a piezometric rise $\Delta h = 0.5$ m causes a 3% drop in factor of safety (see table 10) and that groundwater before the storm was exactly at the level giving $F = 1.0$; $\Delta h'$ will then be equal to the total storm-response rise Δh. Assume also that the relation between s/s_0 and rate of displacement is given by the test results (details in Appendix 4) for weathered Edale Shale shown in figure 24. On day 5, and also day 8, δh is 0.4 m. The drop in factor of safety if the strength remained at s_0 would therefore be 2.4%. Hence the rate of displacement will increase to give a strength ratio s/s_0 equal to 1.024, and from figure 24 this rate is 40 mm day^{-1}. The displacement during each of these days is therefore 0.04 m, and similar calculations applied to the entire period of transient groundwater response give a total displacement $\Delta x = 0.30$ m. Displacements for other values of $\Delta h'$, for six-day storms, are shown in figure 25. It will be seen that the displacement is chiefly concentrated within a few days of the peak rise in piezometric level. This accounts for the occurrence of severe movements at the end of a rainstorm (figure 14).

For a given value of $\Delta h'$ displacement up to the peak is proportional to storm duration, but for a given total storm rainfall the effect of a longer duration is approximately counterbalanced by the correspondingly lower storm-response ratio. Thus 100 mm of rain in six days leads

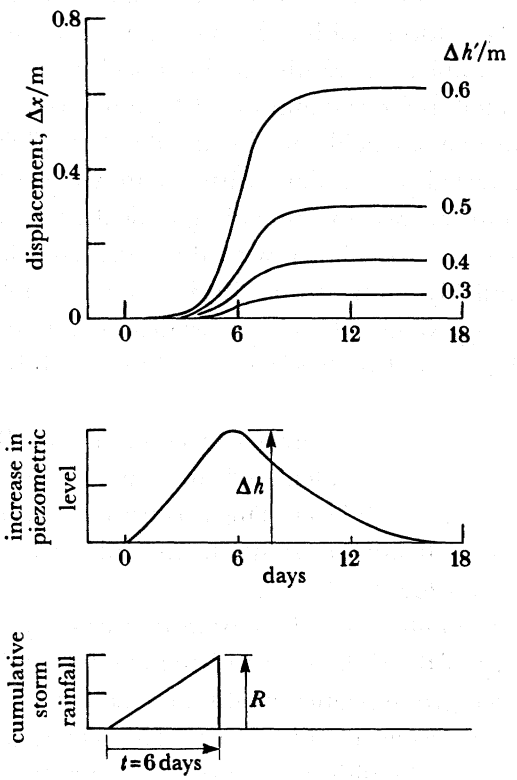

FIGURE 25. Displacements caused by winter rainstorms.

to $\Delta h' = 0.48$ m and $\Delta x = 0.28$ m, whereas 100 mm in 10 days gives $\Delta h' = 0.45$ m and $\Delta x = 0.30$ m.

In the foregoing example, $F = 1.0$ before the rainstorm. This might be the case in a wet winter. More generally, groundwater will be lower than the level giving $F = 1.0$. For instance in a winter of average rainfall it might be 0.2 m below this level, by analogy with observations at Harmondsworth; see §6(*a*). The effective piezometric rise $\Delta h'$ is then less than the full response Δh and no movement will occur until the storm rainfall exceeds 40 mm (assuming $\Delta h/R = 5$). Calculations of Δx proceed as before and show, for a given storm duration, that to a first approximation the displacement is simply a function of $\Delta h'$. Conversely, a small amount of rain following shortly after the major storm can have a disproportionally large effect, as in the later part of December 1965 (figure 14).

TABLE 11. STORM RESPONSE AND DISPLACEMENTS

(Mean values for six-day and 10-day rainstorms.)

storm rainfall	response		displacement Δx			approx. monthly
R/mm	$\Delta h/R$	Δh/m	$\Delta h - \Delta h' = 0$ m	$\Delta h - \Delta h' = 0.1$ m	$\Delta h - \Delta h' = 0.2$ m	rainfall/mm
80	4.5	0.36	0.13	0.04	0.01	150–200
100	4.65	0.46	0.29	0.12	0.04	190–240
120	4.8	0.58	0.60	0.28	0.10	230–280
140	4.9	0.69	1.2	0.60	0.25	270–320

Calculated displacements for Mam Tor landslide are summarized in table 11 as average values for six-day and 10-day storms with $\Delta h - \Delta h'$ varying from 0 to 0.2 m and other assumptions as in the above example. The results can be considered as no more than illustrative but their range, from 0.04 to 0.6 m for 100 mm and 120 mm storms, are of the correct order of magnitude compared to the average field value of about 0.3 m. They also provide a rational basis for the observations recorded in §4. Thus with groundwater 0.2 m or more below the limiting ($F = 1.0$) level, 100 mm storms (corresponding typically to a monthly 200 mm) would produce little or no movement, in accordance with the observed relatively low frequency of slips in response to this rainfall. By contrast, the slip in January 1952, in a month with only 150 mm of rain, was preceded by two months of heavy rain and groundwater before the slip had probably risen to the limiting ($F = 1.0$) level; this would certainly have been the case in February 1966 when 190 mm of rain, following exceptional rainfall and slipping in December 1965, produced 0.3 m displacement. It may further be noted that a 140 mm storm (equivalent to a monthly rainfall of 300 mm) is calculated to cause 0.25 m displacement even if groundwater is 0.2 m below the $F = 1.0$ level. This is consistent with the high probability of slips in winter months of such rainfall, and also with the total absence of slips in summer months when groundwater is always at a low level.

Storm-response movements, totalling less than 10 m in a century at Mam Tor, produce a very small change in geometry of the slide mass and therefore a small change in static factor of safety under normal winter groundwater conditions. Consequently, the process can be repeated many times without any considerable change. Nevertheless, on a long timescale the cumulative effect must be to bring the slide mass into a more stable configuration; F becomes marginally greater and a larger piezometric rise Δh is required to produce a given $\Delta h'$ or displacement. The return period for reactivation is therefore longer and the movement per

century is smaller. Eventually, a state will be reached in which F is sufficiently high for the landslide to remain stable under the heaviest winter rainstorms, and this may be defined as the condition of permanent equilibrium.

11. Evolution of the landslide

Stages in the probable evolution of Mam Tor landslide are sketched in figure 26. This reconstruction is based on the following considerations.

1. To the east of point A, near borehole 4 and about 520 m from the present toe, the slip surface is at a very shallow depth below original ground level. Practically all the slide debris east of this point, including the earthflow, must therefore have been derived from material to the west.

2. For the same reason the initial slip or slips must have been to the west of this point; i.e. in the slump sector.

3. The volume of the initial slip or slips must equal that of the slide debris, after allowing for expansion due to softening and degradation. The 'bulking' factor is approximately 20% in mudstone, 40% in clay matrix and (say) 10% in sandstone.

4. The original profile cannot have been much steeper than the steepest slopes presently existing adjacent to the landslide.

5. The basal slip surface has to pass through the points where it was observed in boreholes 4 and 8, and through the foot of the scarp.

6. The foregoing requirements are satisfied by the profile and slip surface in figure 26*a* with a single large slip rather than several relatively small slips.

7. Shear strength parameters corresponding to a condition of limiting equilibrium before the initial slip are:

Mam Tor Beds	$c' = 20$ kPa	$\phi' = 37°$,
Edale Shales	$c' = 50$ kPa	$\phi' = 26°$.

Other combinations of c' and ϕ' are possible, within limits, but in any case for $F = 1.0$ the mudstone has a shear strength around 200 kPa under an average effective pressure of about 350 kPa. Part of the slip surface passes through weathered mudstone, but when allowance is made for this the unweathered mudstones still has a strength undoubtedly less than the peak value, indicating the effects of long-term creep and progressive failure.

8. Residual strength parameters for sandstone and mudstone are about $\phi'_r = 30°$ and $\phi'_r = 14°$ respectively, with zero cohesion (§8). The post-failure drop in strength therefore amounts to approximately 30% in sandstone and 60% in mudstone.

9. Consequently, the slip mass will undergo large and rapid displacements before reaching a position of (temporary) equilibrium. Such movements in 'brittle' materials are well known. Carsington dam, for instance, moved 13 m in three days before the slip came to rest (Skempton & Coats 1985) and this is a modest example compared to the landslide on the Dorset coast in 1942 (Brunsden & Jones 1976) and several other major slips.

10. Trial-and-error solutions lead to a displacement for the initial Mam Tor slip represented by point B in figure 26*b*. The slide debris is taken as having a volume 15% larger than that of the initial slip, to allow for bulking without a substantial increase in water content, and the factor of safety is 1.0 by using equation (5) with the residual strength parameters given

PHILOSOPHICAL TRANSACTIONS OF THE ROYAL SOCIETY A MATHEMATICAL, PHYSICAL & ENGINEERING SCIENCES

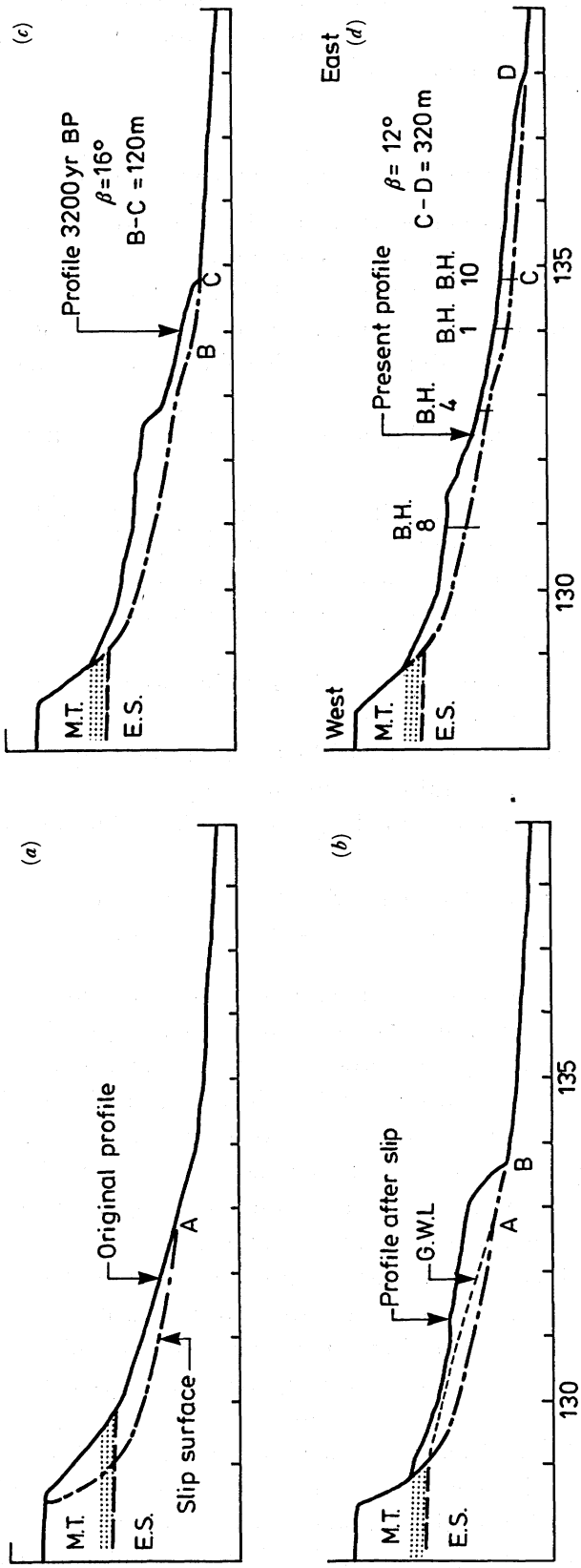

FIGURE 26. Evolution of landslide. (M.T. is Mam Tor Beds, E.S. is Edale Shales.)

PHILOSOPHICAL TRANSACTIONS OF THE ROYAL SOCIETY A MATHEMATICAL, PHYSICAL & ENGINEERING SCIENCES

above and groundwater level as shown. Within the accuracy of the calculations point B is 440 ± 40 m from the present toe.

11. As a result of degradation and softening, secondary slips occur in the lower part of the slump mass leading to the development of an earthflow. For the landslide at Blaina, South Wales, which started in January 1954 in Coal Measures mudstone ($L_1 = 36$, $I_p = 19$) under massive but fractured sandstone beds, this process began almost immediately, as shown by an aerial photograph taken in March 1954 (Skempton & Hutchinson 1969). Moreover, the earthflow advanced about 2 m per year, in winter months, between 1955 and 1980 (Jones & Siddle 1988) with an average slope β from the toe to the scarp foot of about 17°. Winter groundwater levels were high throughout most of the slide mass as a result of flow from an aquifer exposed at the foot of the scarp. The rate is correspondingly high, but not exceptional for 'post-failure' movements (Skempton & Hutchinson 1969), and the Blaina evidence suggests that the rate of advance of the Mam Tor earthflow would initially have been far greater, by roughly one order of magnitude, than the average figure in recent times.

12. The advancing earthflow reached point C, 320 m from the present position of the toe, about 3200 years ago; as demonstrated by the age of an Alder root in a fossil soil beneath the slip surface in borehole 10. At that time $\beta \approx 16°$.

13. Meanwhile, the slump mass itself had been moving, partly as a result of additional weight imposed by scree eroded off the scarp face, and in response to rainfall, but partly also as a result of loss of material from its front edge; for the retrogressing secondary slips apparently remove material at a faster rate than can be supplied by forward movement of the slump.

14. These processes have been operating for about 3600 years, as will be demonstrated, and are still continuing today. Their resultant effect is to bring the landslide into a more stable configuration, and the rate of movement per century will therefore be decreasing: but, clearly, a state of permanent equilibrium has not yet been attained, and the present shape of the landslide, figure 26*d*, with $\beta = 12°$, is merely another stage in a development that will continue for a very long time.

Granted this pattern of evolution it is possible to make an approximate estimate of the date of landslide inception. If at a time T in the past the toe of the earthflow was at a distance X from its present position, any curve relating X and T has to satisfy the conditions

(*a*) at point D, $X = 0$ and $T = 0$ and $\mathrm{d}X/\mathrm{d}T$ equals the present rate of movement (taken as 7 m century^{-1});

(*b*) at point C, $X = 320$ m and $T = 3200$ years,

and by extrapolation to point B, where $X = 440$ m, the time T_1 to the initiation of earthflow movement can be found. For the time–displacement curve shown in figure 27, $T_1 = 3600$ years and $\mathrm{d}X/\mathrm{d}T$ at that time is 0.5 m per year. The initial slip, by comparison, would have been a sudden event. Therefore, T_1 is the estimated date of origin of the landslide.

This estimate is subject to considerable uncertainty arising from possible errors in the assumptions and climatic fluctuation. If the curve in figure 27 is redrawn with the initial rate of movement halved or doubled (to 0.25 or 1.0 m a^{-1}), T_1 becomes 3800 or 3400 years, respectively. If errors in the date at point C (3200 ± 200 years), in the position of point B (440 ± 40 m) and the present rate of movement (say 7 ± 1 m century^{-1}) operate in the same sense their combined effect, given an initial rate of 0.5 m per year, is to produce a variation in T_1 from 3900 to 3200 years. These may be regarded as practical limits. Extreme limits, derived from the improbable case of all four errors operating together in the same sense, are 4300 and 3100 years.

PHILOSOPHICAL TRANSACTIONS OF THE ROYAL SOCIETY A MATHEMATICAL, PHYSICAL & ENGINEERING SCIENCES

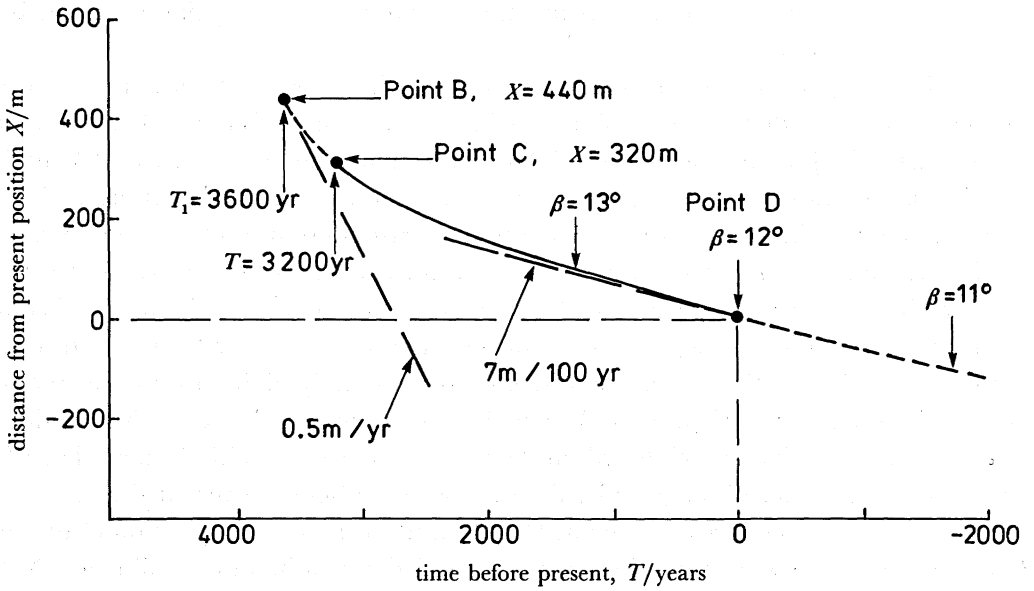

FIGURE 27. Movement of landslide toe ($T = 0$ corresponds to AD 1950).

In summary, the best estimate of the date of landslide inception on this model is about 3600 ± 400 calendar years. From tree-ring calibration (Pearson & Stuiver 1986) the equivalent radiocarbon date is *ca.* 3300 ± 300 years BP.

It could be argued that an upper limit is more acceptable, because ϕ'_r may have been marginally reduced by chemical action subsequent to the initial slip; the value of X at point B would then be greater than 440 m. But, conversely, if movements in the early stages were as fast as those of the Blaina landslide, a lower limit for the date is more appropriate.

Finally, it is interesting to consider the rate of change in geometry of the slide mass, expressed in simple terms by the slope β. At point C, with $T = 3200$ years, β was about 16°. For $\beta = 13°$, $X = 100$ m and $T = 1300$ years, or 2300 years after the initial slip. At the present time $\beta = 12°$ and is decreasing by less than 0.1° per century. For β to fall from 12 to 11°, $X = -100$ m and $T = -1800$ years. At that time, approaching 5500 years after inception, the slide mass would be less sensitive to rainfall, perhaps responding only to very heavy storms; as seems to have been the case at Didsbury Intake where β had exactly this value (§4).

Further extrapolation of the time–displacement curve is not justified, but evidence outlined in the following section indicates that a period of 8000 years may be required for landslides on the scale of Mam Tor to reach permanent equilibrium. The shape of the curve in figure 27 is not inconsistent with $\mathrm{d}X/\mathrm{d}T$ becoming zero after such a time.

12. COMPARATIVE CASES

Information on several Pennine landslides, some considerably older and more stable than Mam Tor, is given by Johnson and his colleagues at Manchester University. Five of these landslides, and another important example in Edale, are briefly described here. Centre-line profiles have been drawn from contours at 10 m intervals as plotted on the 1987 Ordnance Survey 1:25000 map of the northern Peak District. The data are summarized in table 12.

Table 12. Landslides in Namurian Shales

geology	Rough Rock over shale (G_2)	Kinderscout Grit over Grindslow Shale				Mam Tor Beds over Edale Shales	
landslide	Coombes Tor	Tintwistle Knarr	Millstone Rocks	Didsbury Intake	Lawrence Edge	Mam Tor	Mam Nick
length/m	550	850	750	650	1100	1000	1100
height/m	125	240	210	145	270	280	220
scarp: height/m	50	90	70	45	80	80	40
slope	30°	35°	35°	35°	30°	45°	40°
slope from toe to scarp foot, β	9.5°	12.5°	12.5°	11°	11°	12°	10°
approximate age/(calendar years)	>8000	3400	7000	>8200	8300	3600	⩾6600
condition	stable	active	active	nearing stability	stable	active	stable

Coombes Tor (near Charlesworth in Derbyshire; also known as Cown Edge, Coombes Rocks and Far Coombes (Franks & Johnson 1964; Johnson 1965)). This is a slump-earthflow at the head of a wide embayment in the Rough Rock, stratigraphically the highest member of the Namurian Series, overlying mudstones of zone G_1. Sampling in a slip depression in the slump sector, at the position shown in figure 28, revealed peaty deposits 1.8 m thick over 0.15 m of inorganic sediment on slide debris. The basal peat sample can be referred to the top of pollen zone VI because it lies just below the VI–VII boundary, defined principally by a sharp rise in *Alnus*, and the pollen diagram continues upwards in sequence through zones VIIa, VIIb and VIII. The VI–VII boundary has been dated around 7100 radiocarbon years BP at two north of England sites: Scaleby Moss, Cumbria (Godwin *et al.* 1957) and Red Moss, Lancashire (Hibbert *et al.* 1971). If the age of the basal peat sample is taken as 7200 radiocarbon years or 8000 calendar years BP (see Appendix 2), this will be a minimum date for landslide inception, because the slip must have started before the depression was formed and there would be a further interval before peat become established.

At Coombes Tor, $\beta = 9.5°$ and the scarp slope is about 30°. The slide appears to be stable; in particular the earthflow sector has long been converted to smooth permanent pasture. These characteristics are in contrast to the much younger and still active Mam Tor landslide, with its steep scarp and hummocky earthflow, where $\beta = 12°$.

Didsbury Intake (on the north side of Longdendale, above Rhodes Wood dam (Tallis & Johnson 1980)). This is the ancient landslide mentioned in §4 as having been reactivated by very heavy rain in February 1852. It was subsequently stabilized by deep drainage adits (Bateman 1884). The geological succession here consists of Kinderscout Grit over Grindslow Shale (base of the middle Namurian) over Shale Grit sandstone, the latter limiting the depth of slip surface and forming a steep slope above river level (figure 28).

Pollen analysis of a peaty deposit in a depression in the slump sector shows a continuous diagram from zone VI up to zone VIII. The basal peat sample is referred to the upper part of zone VI, distinctly below the VI–VII boundary. Its age, and therefore a minimum age for the landslide, may be taken as about 7400 radiocarbon years, this being the date of peat samples occupying a comparable position in the pollen diagrams at Red Moss and Scaleby Moss.

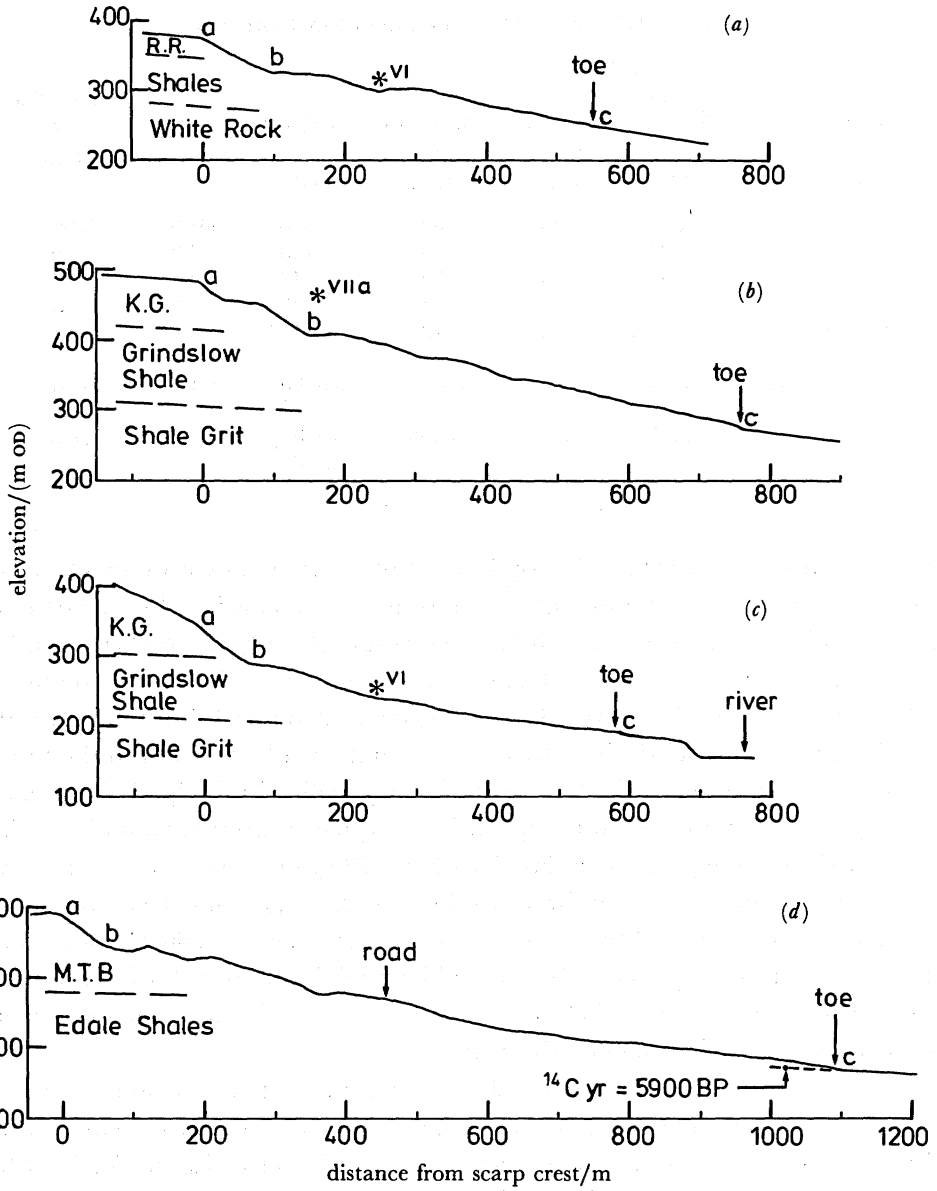

FIGURE 28. Landslide profiles. (*a*) Coombes Tor; $\beta = 9.5°$ (average slope from b to c). (R.R. = Rough Rock.) (*b*) Millstone Rocks; $\beta = 12.5°$. (K.G. = Kinderscout Grit.) (*c*) Didsbury Intake; $\beta = 11°$. (*, pollen samples.) (*d*) Mam Nick; $\beta = 10°$. (M.T.B. = Mam Tor Beds.)

The slide mass, with $\beta = 11°$, clearly had not yet reached a state of permanent equilibrium before the nineteenth-century stabilization works; but it was reactivated only by rainfall corresponding to a return period of the order of 50 years (§6).

Tintwistle Knarr (on the north side of Longdendale, above Rhodes Wood reservoir (Tallis & Johnson 1980)). Though adjacent to Didsbury Intake, in very similar geological conditions, the landslide at Tintwistle Knarr is larger and more recent. A basal peat sample in a depression at the scarp foot was formed later than the rise in *Calluna* pollen, dated between 4400 and 3700 radiocarbon years at four sites in Lancashire, Yorkshire and Derbyshire (Hibbert *et al.* 1971; Bartley 1975; Tinsley 1975; Hicks 1971), and before the forest clearance horizon dated

2400–2200 radiocarbon years at three of these sites and another in Derbyshire (Tallis & Switsur 1973). The landslide therefore appears to be approximately similar in age to the Mam Tor slip. The slide mass stands at $\beta = 12.5°$, with very irregular topography, and an earthflow in the lower part, sloping at 12°, is recorded as having moved about 1 m in 13 years (Bateman 1884; see §4).

Millstone Rocks (on the north side of Longdendale about 1.5 km from Didsbury Intake, at a higher elevation (Johnson & Walthall 1979)). Like Mam Tor, the Millstone Rocks landslide is a slump-earthflow at the head of a valley, in this case the valley of a tributary stream running into Longdendale below Torside dam. However, the earthflow is restricted from expanding laterally and becomes narrower, rather than wider, towards the toe.

The basal peat sample in a slip depression at the scarp foot (figure 28) can be referred to the early part of pollen Zone VII a. This zone extends in time from 7100 radiocarbon years (as mentioned above) to a well-defined limit at 5000 years marked principally by a decline in *Ulmus* pollen (see, for example, Godwin 1960; Hibbert *et al.* 1971; Hicks 1971). Peat at this location probably began forming not long after the initial slip, and if so the landslide can be dated, in round figures, to 6500 radiocarbon years or 7000 calendar years BP.

The slide is still active; perhaps as active as Mam Tor landslide. This observation accords with the relatively high value of $\beta = 12.5°$ but leaves a discrepancy between the date of origin and that of Mam Tor and Tintwistle Knarr. A possible explanation may be sought in the restraint offered to movement of the earthflow by the valley configuration at Millstone Rocks.

Lawrence Edge (on the south side of Longdendale at Woodhead dam (Johnson & Walthall 1979; Tallis & Johnson 1970)). Here the Grindslow Shale extends down to the valley floor and the toe of the landslide was revealed at river level, while excavating the cut-off trench of Woodhead dam, as 'slipped shale' 12–15 m thick (Bateman 1884). Pollen analyses of samples from peat-filled hollows at three different elevations show that this massive landslide developed as a series of retrogressive slips, possibly initiated by river erosion and occurring intermittently over a period of at least 5000 years from about 7500 radiocarbon years BP. It therefore represents a type different from the slump-earthflows, but is of interest in the present context as providing a dated example of a large landslide that is at or close to a state of permanent equilibrium. From the toe (as shown in Bateman's section of the cut-off trench) up to the scarp foot $\beta = 11°$ and the slope, though displaying unmistakeable landslide topography, has undergone no significant mass movement for some considerable time.

Mam Nick landslide, on the south side of Edale, extends from a well-defined toe 30 m above river level up to a scarp in the hog-back sandstone ridge (Rushup Edge) running west from Mam Tor, and about 1 km from Mam Tor landslide. Geologically, the two sites are similar and the landslides are comparable in size, but in other respects they exhibit strong contrasts. At Mam Nick $\beta = 10°$, the scarp face is grass-covered, a road crossing the slide has shown no signs of movement for many years (even in the exceptional rainfall of December 1965) and the main stream carrying surface run-off has eroded a gully through the lower part of the earthflow. These features indicate stable conditions characteristic of an old landslide; and a much greater age, relative to Mam Tor, is confirmed by a radiocarbon date of 5860 ± 120 years (*ca.* 6600 calendar years BP) on charcoal fragments disseminated in a fossil soil exposed in the gully, under 10 m of slide debris, less than 100 m from the toe (Brown & Redda 1989). The landslide might have started at least 2000 years before that date.

Comparison between these cases cannot be exact, but broadly it appears that large landslides

in Namurian mudstones remain unstable if β exceeds about 10 or 11°, and that a period of the order of 8000 years is required for such landslides to attain a state of permanent equilibrium. Weathering and soil creep will of course continue long afterwards.

13. Summary and conclusions

Investigations at Mam Tor provide data for a quantitative assessment of the process governing the evolution of a massive landslide of the slump-earthflow type. About 3200 years ago the slope β, from the toe to the scarp foot, was approximately 16°. Since that time the toe has advanced 320 m at an average rate of 10 m per century and today, some 3600 years after landslide inception, $\beta = 12°$ and the slide mass is close to equilibrium under normal winter groundwater conditions. But at four-year intervals, on average, it is reactivated by a transient rise of water level in response to winter rainstorms typically exceeding 100 mm in 10 days (characteristic of 200 mm monthly rainfall). As a result of a succession of small displacements in each rainstorm the toe is now advancing at about 7 m century^{-1} and as it does so the slide mass moves into a slightly more stable position, requiring heavier rain and a longer return period for its reactivation. Consequently, the long-term rate of movement is slowly decreasing, and eventually the landslide will reach a state in which equilibrium can be maintained under the heaviest rainfall. This process, operating in the past, appears to have been completed in some other large Pennine landslides after a period of not less than 8000 years (or 7200 radiocarbon years) with β reduced to about 10°.

The present state of limiting equilibrium at Mam Tor corresponds to a static residual strength in the clay (degraded mudstone) in the basal shear zone represented by an angle of shearing resistance $\phi'_r = 14°$; a figure in good agreement with tests on clays of similar composition. The intermittent displacements can be modelled by an analysis based on the transient rise of groundwater level, inferred from observed storm-response ratios in clay soils, and laboratory measurements of the increase in residual strength with increasing rates of shear.

The paper is published by permission of Derbyshire County Council. Imperial College funded the radiocarbon assays. Dr W. H. C. Ramsbottom, of the British Geological Survey, carried out the palaeontological determinations and Mr D. J. Lowe, also of BGS, gave valuable assistance in describing the rock cores. We thank Dr I. P. Stevenson for help in geological interpretations, Professor R. G. West, F.R.S., for the pollen analysis, and Professor P. R. Vaughan for important contributions to the analysis of storm response mechanics. Dr R. H. Johnson kindly read the manuscript and made helpful comments based on his experience with Pennine landslides. Grateful acknowledgement is made to Mr R. D. Brown of Sheffield University for access to observations of the movements at Mam Tor in 1965–66 and information, as yet unpublished, on the Mam Nick landslide. Soil Mechanics Ltd carried out the boreholes and piezometer installations.

PHILOSOPHICAL TRANSACTIONS OF THE ROYAL SOCIETY A MATHEMATICAL, PHYSICAL & ENGINEERING SCIENCES

Appendix 1. Pollen analysis

From the peaty soil in borehole 10, depth 19.3–19.45 m, two samples were taken; one for pollen analysis, the other for radiocarbon dating. Results of the pollen analysis by Mrs S. Peglar under the direction of Professor R. G. West, Botany School, University of Cambridge, are given below.

Betula	Birch	no. of grains = 103
Pinus	Pine	1
Ulmus	Elm	3
Quercus	Oak	109
Tilia	Lime	1
Alnus	Alder	600
Fraxinus	Ash	1
Corylus	Hazel	103
Salix	Willow	3
Ilex	Holly	15
		939

Gramineae	Grass	no. of grains = 24
Plantago	Plantain	1
Ranunculus	Buttercup	1
Rosaceae	Rose	4
Ulex	Furze	1
		31
Sphagnum	Moss	5
Filicales	Ferns	7
Pteridium	Bracken	2
		14

total = 984

In a letter to the senior author, dated 5 August 1980, Professor West comments that 'the high frequency of *Alnus* and the sediment type (wood peat) indicate local fen carr. *Betula*, *Quercus* and *Corylus* are also present in considerable frequency, the first two possibly associated with carr. The age of the assemblage is probably Godwin's zone VIIb, since although only one *Plantago lanceolata* grain was recorded in the count, others were seen in scanning, and the *Ulmus* frequency is low.'

Pollen zone VIIb ranges in date from about 5000 to 2500 radiocarbon years BP (Godwin 1960). The date of 3910 ± 60 years for this soil (Appendix 2) is therefore conformable to the age suggested on botanical evidence.

Appendix 2. Radiocarbon dating

The following assays were made by Dr R. E. G. Williams at the Radiocarbon Dating Laboratory, University of Birmingham. Ages are given in radiocarbon years BP (AD 1950) assuming a constant ^{14}C half-life of 5568 years. Also given are the equivalent ages in calendar years and, in brackets, the range corresponding to one standard deviation; from definitive calibration curves based on tree-ring dating (Stuiver & Pearson 1986; Pearson & Stuiver 1986).

Sample 1. Borehole 4, depth 9.5 m.
Alder root in landslide debris
Pretreatment: 5% HCl and 2% NaOH
Age: 860 ± 100 years
Reference number: Birm – 1061
Cal yrs BP = 770 (920–690)

Sample 2. Borehole 10, depth 19.35 m.
Alder root from peaty soil beneath landslide
Pretreatment: 5% HCl and 2% NaOH
Age: 2970 ± 150 years
Reference number: Birm – 1062
Cal yrs BP = 3190 (3360–2950)

Sample 4A. Borehole 10, depth 19.3–19.45 m.
Wood fragments from peaty soil
Pretreatment: soil broken down with 6N HCl, wood fragments sieved out and treated with 0.1% NaOH
Age: 3080 ± 120 years
Reference number: Birm – 1078A
Cal yrs BP = 3310 (3450–3160)

Sample 4B. Borehole 10, depth 19.3–19.45 m.
Peaty soil, fine fraction
Pretreatment: 6N HCl
Age: 3910 ± 60 years
Reference number: Birm – 1078B
Cal yrs BP = 4390 (4430–4250)

Calibration

Calibration of the radiocarbon timescale by tree-ring dating is now established with a probable error of about ±25 years to 4000 BP and with less precision to 8000 BP. Thereafter calibrations can be derived from varve chronology. Table 13 gives a summary of data presented at the Twelfth International Radiocarbon Conference (Stuiver & Kra 1986) and by Bjorck *et al.* (1987).

TABLE 13. CALIBRATION OF RADIOCARBON TIMESCALE

(Dates in years BP.)

radiocarbon	calendar	radiocarbon	calendar
1000	950	6000	6800
2000	1950	7000	7800
3000	3200	8000	8800
4000	4400	9000	9700
5000	5700	10000	10600

APPENDIX 3. STORM-RESPONSE DATA

Information on storm response in clay soils can be derived from observations recorded by Black *et al.* (1958) for sites at Harmondsworth and Uxbridge, and from investigations of landslides at Burderop Wood, near Swindon (Skempton 1972), at Bredon Hill (Skempton & Henkel 1958) and in San Martino valley (Bertini *et al.* 1984). A brief description of the sites is given in §6*b* of the paper, but because such data have not previously been published the relevant details are given in table 14.

TABLE 14. WINTER STORM RESPONSE AND RAINFALL

location	strata	depth to winter GWL/m	typical seasonal response/m	storm: date	storm: rain R/mm	storm: duration days	storm: intensity (mm day^{-1})	storm response Δh/m	$\Delta h/R$
Harmondsworth[a] (level site)	sandy clay ($L_1 = 36$) over clayey gravel	2.6	0.9	Nov. 51	72	9	8	0.46	6.4
				Mar. 52	40	7	6	0.27	6.7
				Dec. 52	52	14	4	0.30	5.8
				Nov. 54	114	17	7	0.73	6.4
Uxbridge[a] (4° slope)	silty clay ($L_1 = 55$–88)	0.3	1.0	Nov. 54	70	8	9	0.30	4.3
				Jan. 56	53	8	7	0.21	4.0
Burderop Wood[b] (6° slope)	Colluvial Gault ($L_1 = 71$)	1.4	0.6	Jan. 71	92	14	7	0.28	3.0
				Nov. 71	55	14	4	0.20	3.6
Bredon Hill[c] (12° slope)	Colluvial Lias ($L_1 = 66$)	0.7	1.1	Feb. 57	65	14	5	0.34	5.2
San Martino[d] (9° slope)	Colluvial silty clay ($L_1 = 42$)	0.6	1.6	Mar. 82	170	18	9	0.95	5.6

[a] Covered borehole. [b] Piezometers at 4 m.
[c] Piezometers at 2 m. [d] Piezometers at 5 and 15 m.

Appendix 4. Residual strength tests

Values of the residual strength parameter ϕ'_r plotted in figure 22 have mostly been determined from tests on a natural slip surface in samples taken from a landslide or from strata sheared tectonically. An alternative procedure, which can be used where slip surface samples are not available, is to cut a plane in the specimen and then subject it to multiple reversals in a shear box. When successful, such tests give a constant and repeatable minimum strength after five or six reversals. Typical examples of slip surface and cut-plane tests and notes on all but two of the sites listed in figure 22 are given by Skempton (1985). Slip surface tests on a Lower Devonian mudstone from a landslide near Monmouth are recorded by Petley (1966) and the location is described by Early & Jordan (1985). The other additional site is Carsington dam in Derbyshire, where a slip occurred during construction (Skempton & Coats 1985). Of particular interest in the present context are tests on the Carsington slip surface in mudstone fill. The fill material was obtained from borrow pits in slightly weathered Edale Shales; it was acidic, as a result of pyrite oxidation, and had been in place for two years when sampled, and its index properties are similar to those of the shear zone clay at Mam Tor. The tests, carried out at a rate of displacement of 2 mm day^{-1}, gave highly consistent results with ϕ'_r just under 15°.

To include materials of very low or zero plasticity three points have been added: for a uniform and a well-graded sand (Lupini 1980) and for amorphous silica containing a high proportion of fine particles but no clay minerals (Kenney 1967).

All the tests on clays summarized in figure 22 were made at 'slow' rates of displacement, between 2 and 10 mm day^{-1}. Special tests to determine the 'static' residual strength, and also to extend measurements into a range above the usual laboratory rates, have been carried out at Imperial College on London Clay (Petley 1966) and completely weathered Edale Shale (D. J. Petley, personal communication). The procedure is to establish a well-defined residual strength in cut-plane tests using a 'standard' rate, in this case 1.5 mm day^{-1}, and then to apply a faster or slower rate, returning to the standard after each application. Four virtually identical samples were tested with eight measurements at each rate to obtain reasonably accurate values of the small differences involved. The results are expressed as ratios of strength at a given rate to that of the standard. When plotted against rate of displacement on a logarithmic scale a marked decrease in gradient is found as the rate decreases, and extrapolation permits a close estimate to be made of the 'static' strength corresponding to effectively a zero rate which, in practice, can be taken as 0.01 mm day^{-1}. The strength ratios are then recalculated in terms of this static value, the results being shown in figure 24.

The samples of brown London Clay were prepared from blocks of material taken at a depth of 5 m from a site at Hendon in north London, and the tests cover a range of rates from 0.06 to 150 mm day^{-1}. This is a clay of high plasticity ($I_p = 49$) containing about 60% of particles smaller than 0.002 mm. The other material tested by Petley is a more sandy clay of completely weathered Edale Shale, or possibly Head derived from it, sampled at a depth of 0.6 m in an 8° slope near Atlow village, Derbyshire, 6 km east of Ashbourne. This provides useful data for Mam Tor because the index properties are comparable with those of the shear-zone material of the landslide, as seen from table 8.

PHILOSOPHICAL TRANSACTIONS OF THE ROYAL SOCIETY A MATHEMATICAL, PHYSICAL & ENGINEERING SCIENCES

References

Babtie Shaw and Morton & Skempton, A. W. 1986 *Carsington dam investigation; the mechanism of failure.* Report to Severn-Trent Water Authority.

Bartley, D. D. 1975 Pollen analytical evidence for prehistoric forest clearance in the upland area west of Rishworth, West Yorkshire. *New Phytol.* **74**, 375–381.

Bateman, J. F. 1884 *History and description of the Manchester Waterworks.* Manchester and London: Day and Spon.

Bertini, T., Cugusi, F., D'Elia, B. & Rossi-Doria, M. 1984 Climatic conditions and slow movements of colluvial covers in central Italy. *Proc. 4th Int. Symp. Landslides* **1**, 367–376.

Black, W. P. M., Croney, D. & Jacobs, J. C. 1958 Field studies of the movement of soil moisture. *Road Research Tech. Paper no. 41.* London: HMSO.

Bjorck, S., Sandgren, P. & Holmquist, B. 1987 A magnetostratigraphic comparison between ^{14}C years and varve years during the Late Weichselian. *J. Quaternary Science* **2**, 133–140.

Brown, R. D. 1966 Recent landsliding at Mam Tor. *Don* (Journal of Sheffield University Geographical Society) no. 10, 13–18.

Brown, R. D. & Redda, A. 1989 (In preparation.)

Brunsden, D. & Jones, D. K. C. 1976 The evolution of landslide slopes in Dorset. *Phil. Trans. R. Soc. Lond.* A **283**, 605–631.

Burek, C. V. 1985 The Bakewell till. *Peak District & Northern Dukeries* (ed. D. J. Briggs, D. D. Gilbertson & R. D. S. Jenkinson), pp. 43–70. (Quaternary Research Association Field Guide.)

Casagrande, A. 1947 Classification and identification of soils. *Proc. Am. Soc. civ. Engrs* **73**, 783–810.

Casagrande, A. 1949 Soil mechanics in the design and construction of the Logan Airport. *J. Boston Soc. civ. Engrs* **36**, 192–221.

Early, K. R. & Jordan, P. G. 1985 Some landslipping encountered during construction of the A40 near Monmouth. *Q. Jl Engng Geol.* **18**, 207–224.

Flood Studies Report 1975 *Hydrological data*, vol. 4. London: Natural Environment Research Council.

Franks, J. W. & Johnson, R. H. 1964 Pollen analytical dating of a Derbyshire landslip: the Cown Edge landslides, Charlesworth. *New Phytol.* **63**, 209–216.

Geological Survey 1977 *Quaternary map of the United Kingdom* (1 inch to 10 miles).

Godwin, H. 1960 Radiocarbon dating and Quaternary history in Britain. *Proc. R. Soc. Lond.* B **153**, 287–320.

Godwin, H., Walker, D. & Willis, E. H. 1957 Radiocarbon dating and post-glacial vegetational history: Scaleby Moss. *Proc. R. Soc. Lond.* B **147**, 352–366.

Hibbert, F. A., Switsur, V. R. & West, R. G. 1971 Radiocarbon dating of Flandrian pollen zones at Red Moss, Lancashire. *Proc. R. Soc. Lond.* B **177**, 161–176.

Hicks, S. P. 1971 Pollen-analytical evidence for the effect of prehistoric agriculture on the vegetation of north Derbyshire. *New Phytol.* **70**, 647–667.

Hutchinson, J. N. 1969 A reconsideration of the coastal landslides at Folkestone Warren, Kent. *Géotechnique* **19**, 6–38.

Insley, H. & McNicholl, D. 1982 Groundwater monitoring of a soil slope in Hong Kong. *Proc. 7th Southeast Asia Geotech. Conf.*, pp. 63–75.

Johnson, R. H. 1965 A study of the Charlesworth landslides near Glossop, north Derbyshire. *Trans. Inst. Br. Geogrs* **37**, 111–126.

Johnson, R. H. & Walthall, S. 1979 The Longdendale landslides. *Geol. J.* **14**, 135–158.

Jones, D. B. & Siddle, H. J. 1988 Geotechnical parameters for stabilisation measures to a landslide. *Proc. 5th Int. Symp. Landslides* **1**, 193–198.

Kenney, T. C. 1967 The influence of mineral composition on the residual strength of natural soils. *Proc. Geotech. Conf., Oslo* **1**, 123–129.

Lupini, J. F. 1980 The residual strength of soils. Ph.D. thesis, University of London, U.K.

Pearson, G. W. & Stuiver, M. 1986 High-precision calibration of the radiocarbon time scale, 500–2500 B.C. *Radiocarbon* B **28**, 839–862.

Petley, D. J. 1966 The shear strength of soils at large strains. Ph.D. thesis, University of London, U.K.

Sarma, S. K. 1973 Stability analysis of embankments and slopes. *Géotechnique* **23**, 423–433.

Skempton, A. W. 1953 The colloidal activity of clays. *Proc. 3rd Int. Conf. Soil Mech. Fdn Engng* **1**, 57–61.

Skempton, A. W. 1972 Investigations and remedial works at Burderop Wood and Hodson landslides on the M4 Motorway near Swindon. Report to Sir Alexander Gibb & Partners.

Skempton, A. W. 1985 Residual strength of clays in landslides, folded strata and the laboratory. *Géotechnique* **35**, 3–18.

Skempton, A. W. & Coats, D. J. 1985 Carsington dam failure. In *Failures in Earthworks*, pp. 203–220. London: Institution of Civil Engineers.

Skempton, A. W. & Henkel, D. J. 1958 *Landslips and remedial works on Bredon Hill.* Report to Coventry Corporation.

Skempton, A. W. & Hutchinson, J. N. 1969 Stability of natural slopes and embankment foundations. *Proc. 7th Int. Conf. Soil Mech. Fdn Engng* **2**, 291–340.

PHILOSOPHICAL TRANSACTIONS OF THE ROYAL SOCIETY A MATHEMATICAL, PHYSICAL & ENGINEERING SCIENCES

Stevenson, I. P. 1972 Geological Sheet SK18SW (6 inches to a mile). British Geological Survey.
Stevenson, I. P. & Gaunt, G. D. 1971 *Geology of the country around Chapel en le Frith*. Memoir, British Geological Survey.
Stevenson, I. P. & Gaunt, G. D. 1975 Geological Sheet SK18 (1:25000) *Castleton*. British Geological Survey.
Steward, N. E. & Cripps, J. C. 1983 Some engineering implications of chemical weathering of pyrite shale. *Q. Jl Engng Geol.* **16**, 281–289.
Stuiver, M. & Kra, R. (eds) 1986 *Proc. 12th Int. Radiocarbon Conf. Radiocarbon* B **28**, 801–1030.
Stuiver, M. & Pearson, G. W. 1986 High-precision calibration of the radiocarbon time scale, AD 1950–500 BC. *Radiocarbon* B 28, 805–838.
Tallis, J. H. 1964 The pre-peat vegetation of the southern Pennines. *New Phytol.* **63**, 363–373.
Tallis, J. H. & Johnson, R. H. 1980 The dating of landslides in Longdendale, north Derbyshire, using pollen-analytical techniques. *Timescales in geomorphology* (ed. R. A. Cullingford, D. A. Davidson & J. Lewin), pp. 189–205. Chichester: Wiley.
Tallis, J. H. & Switsur, V. R. 1973 Studies on southern Pennine peats. A radiocarbon-dated pollen diagram from Featherbed Moss, Derbyshire. *J. Ecol.* **61**, 743–751.
Terzaghi, K. & Peck, R. B. 1948 *Soil mechanics in engineering practice*. New York: Wiley.
Tinsley, H. M. 1975 The former woodland of Nidderdale Moss, Yorkshire. *J. Ecol.* **63**, 1–26.
Varnes, D. J. 1958 Landslide types and processes. In *Landslides and engineering practice* (ed. E. B. Eckel), Special Rep. no. 29, pp. 20–47. Washington, D.C.: Highway Research Board.
Vear, A. & Curtis, C. 1981 A quantitative evaluation of pyrite weathering. *Earth Surface Processes Landforms* **6**, 191–198.

PHILOSOPHICAL TRANSACTIONS OF THE ROYAL SOCIETY A MATHEMATICAL, PHYSICAL & ENGINEERING SCIENCES

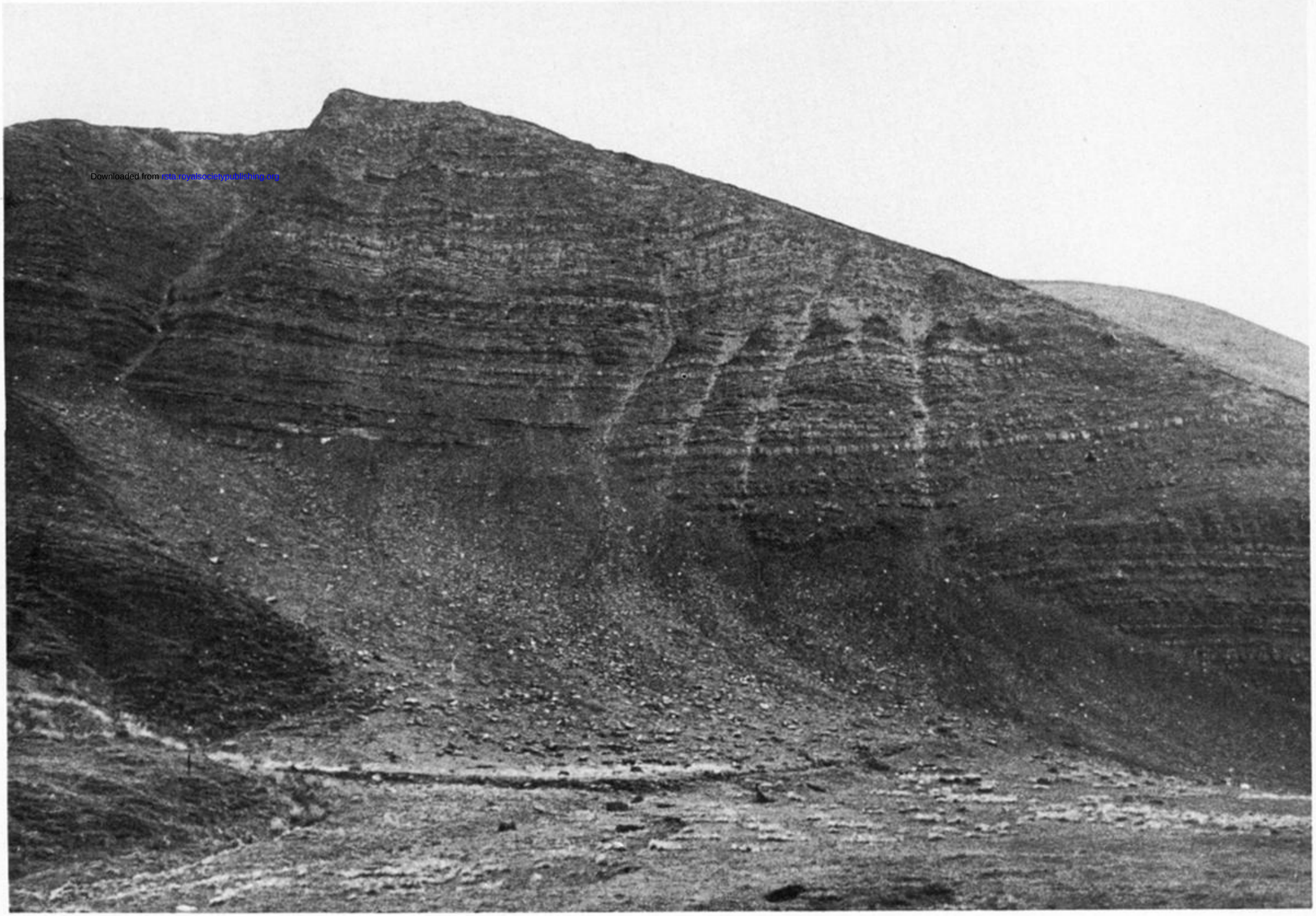

FIGURE 6. Scarp and scree slope.

PHILOSOPHICAL TRANSACTIONS OF THE ROYAL SOCIETY A MATHEMATICAL, PHYSICAL & ENGINEERING SCIENCES

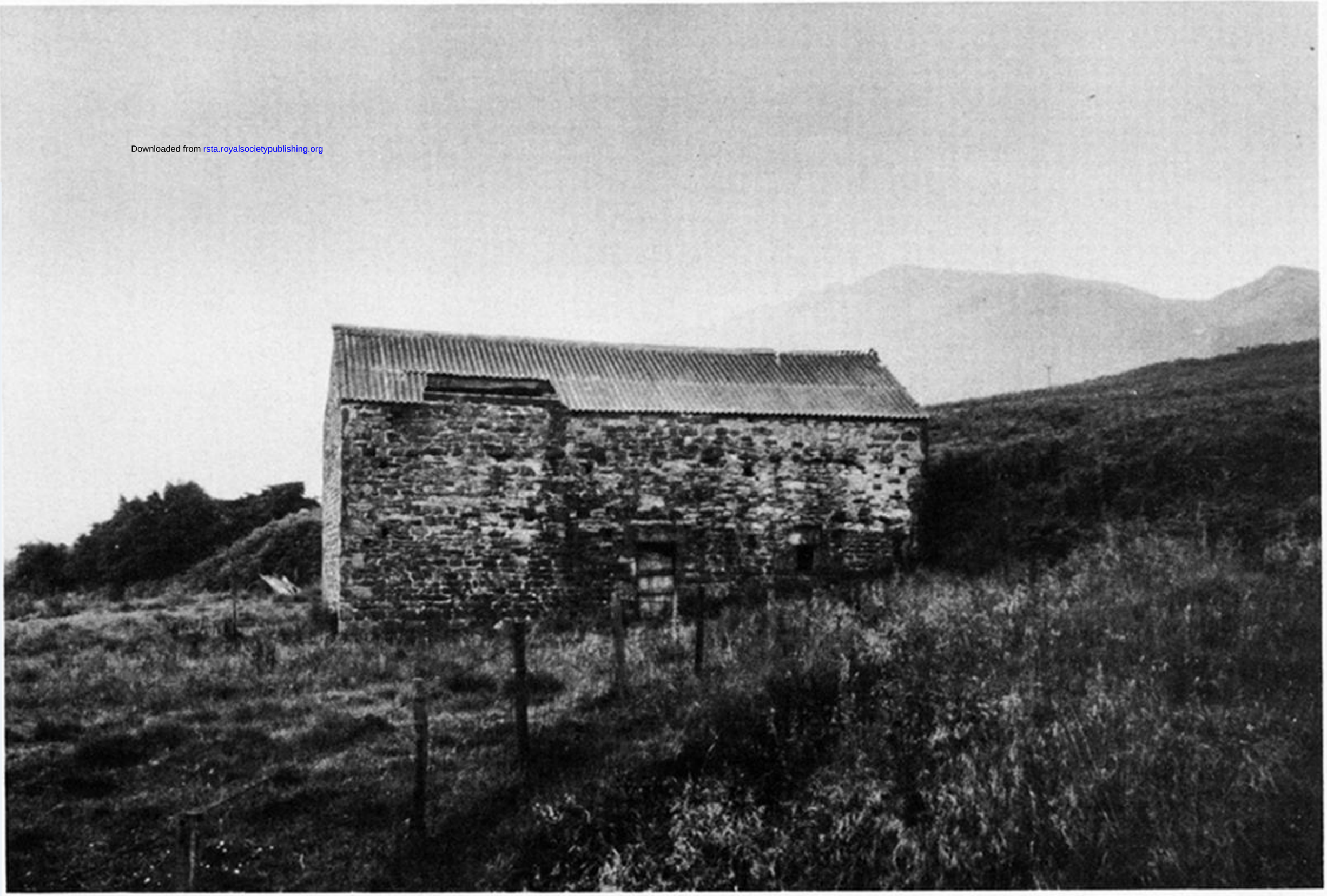

FIGURE 10. Toe of earthflow at Blacketlay Barn.

PHILOSOPHICAL TRANSACTIONS OF THE ROYAL SOCIETY A MATHEMATICAL, PHYSICAL & ENGINEERING SCIENCES

FIGURE 7. Views of landslide, looking south.

PHILOSOPHICAL TRANSACTIONS OF THE ROYAL SOCIETY A MATHEMATICAL, PHYSICAL & ENGINEERING SCIENCES